chemosensors

MDPI

Review

Advanced NIR-II Fluorescence Imaging Technology for Precise Evaluation of Nanomedicine Delivery in Cancer Therapy

Meng Li [1,2], Tuanwei Li [1], Feng Wu [1], Feng Ren [1], Sumei Xue [1] and Chunyan Li [1,3,*]

[1] CAS Key Laboratory of Nano-Bio Interface, Division of Nanobiomedicine and *i*-Lab, Suzhou Institute of Nano-Tech and Nano-Bionics, Chinese Academy of Sciences, Suzhou 215123, China; mli2022@sinano.ac.cn (M.L.); twli2020@sinano.ac.cn (T.L.); fwu2019@sinano.ac.cn (F.W.); fren2021@sinano.ac.cn (F.R.); smxue2023@sinano.ac.cn (S.X.)

[2] State Key Laboratory of Natural Medicines, Jiangsu Key Laboratory of Drug Discovery for Metabolic Diseases, Center of Advanced Pharmaceuticals and Biomaterials, China Pharmaceutical University, Nanjing 210009, China

[3] Key Laboratory of Precision and Intelligent Chemistry, University of Science and Technology of China, Hefei 230026, China

* Correspondence: cyli2012@sinano.ac.cn

Abstract: Tumors represent a significant threat to human health, underscoring the critical need for effective treatment strategies. However, conventional drug therapies are hampered by imprecise delivery, potentially leading to inadequate efficacy and severe side effects. The strategic development of nanomedicines is believed to harbor enormous potential for enhancing drug safety and efficacy, especially for precise, tumor-targeted therapies. Nevertheless, the fate of these nanomedicines within the human body is intricately governed by various physiological barriers and complex environments, posing challenges to predicting their behaviors. Near-infrared II (NIR-II, 1000–1700 nm) fluorescence imaging technology serves as a non-invasive, real-time monitoring method that can be applied for the precise evaluation of nanomedicine delivery in cancer therapy due to its numerous advantages, including high tissue penetration depth, high spatiotemporal resolution, and high signal-to-noise ratio. In this review, we comprehensively summarize the pivotal role of NIR-II fluorescence imaging in guiding the intratumoral precise delivery of nanomedicines and shed light on its current applications, challenges, and promising prospects in this field.

Keywords: nanomedicine; NIR-II fluorescence imaging; nanomedicine delivery; cancer therapy

Citation: Li, M.; Li, T.; Wu, F.; Ren, F.; Xue, S.; Li, C. Advanced NIR-II Fluorescence Imaging Technology for Precise Evaluation of Nanomedicine Delivery in Cancer Therapy. *Chemosensors* **2024**, *12*, 113. https://doi.org/10.3390/chemosensors12060113

Received: 3 April 2024
Revised: 12 June 2024
Accepted: 14 June 2024
Published: 16 June 2024

1. Introduction

Cancer, the most fatal disease globally, represents a significant threat to human health. In 2020, there were an alarming 19.3 million new cases and 10.0 million deaths attributed to cancer [1]. Notably, as a disease associated with aging, cancer prevalence is particularly pronounced in China, home to the world's largest aging population and grappling with an unprecedented aging crisis. In 2020, nearly a quarter of all new cancer cases globally and approximately 30% of cancer-related deaths were reported in China [2]. Similarly, in other regions, the burden of cancer is immense. For instance, in the United States in 2023, there were 5370 new cancer cases and 1670 cancer-related deaths each day [3]. Despite significant advances in traditional cancer treatment, including surgery, chemotherapy, and radiation therapy, cancer remains a formidable global health challenge, becoming an increasingly substantial burden around the world.

In recent years, rapid progress in nanotechnology and biomaterials science has paved the way for nano-based strategies for precise, tumor-targeted drug therapy. There are several key advantages of nanomedicine delivery systems: (1) Enhanced bioavailability: nanomedicines can significantly improve the solubility and stability of drugs within the body, thereby enhancing their bioavailability. (2) Targeted delivery: nanomedicines can

specifically recognize and bind to diseased cells and tissues by surface modification, achieving targeted delivery and minimizing the impact on normal cells, thereby reducing side effects. (3) Controlled release: nanomedicines can achieve the controlled and sustained release of drugs, maintaining the drug concentration within the therapeutic window over an extended period, thereby enhancing efficacy and reducing the frequency of dosing. (4) Multifunctionality: nanomedicines can integrate therapeutic and diagnostic functions into one system. This integration, known as "theranostics", allows for simultaneous drug delivery and imaging [4]. Nanomedicine delivery systems have shown great potential to improve the effectiveness of treatments and reduce adverse reactions [5].

Despite their potential, nanomedicines face significant challenges both in their development and within the body. Key factors are related to their engineering, preparation, stability, and storage. More importantly, they continue to encounter significant challenges within the body due to tumor heterogeneity and a complex biological environment. These include rapid clearance from the bloodstream, low accumulation at tumor sites, limited penetration into deep tumor tissues, and ineffective cellular internalization [6]. To overcome these hurdles, imaging strategies are crucial for monitoring and guiding the design and optimization of nanomedicines [7]. These imaging technologies include magnetic resonance imaging (MRI), computed tomography (CT), positron emission tomography (PET), single-photon emission computed tomography (SPECT), and ultrasound imaging (US) [8]. However, these imaging techniques have drawbacks. CT and MRI typically require high doses of contrast agents. PET and SPECT require the use of radioactive tracers, which pose safety risks. Moreover, these imaging modalities usually involve lengthy image acquisition and post-processing processes, making real-time imaging unachievable. Fluorescence imaging with high sensitivity, fast feedback, multiplexing, and the absence of ionizing radiation overcomes the above-mentioned limitations and exhibits great potential for the evaluation of nanomedicine delivery in vivo [9,10]. Especially notable is deep-tissue fluorescence imaging in the second near-infrared window (NIR-II, 1000–1700 nm), a new optical transparency window for biological tissues (Figure 1) [11].

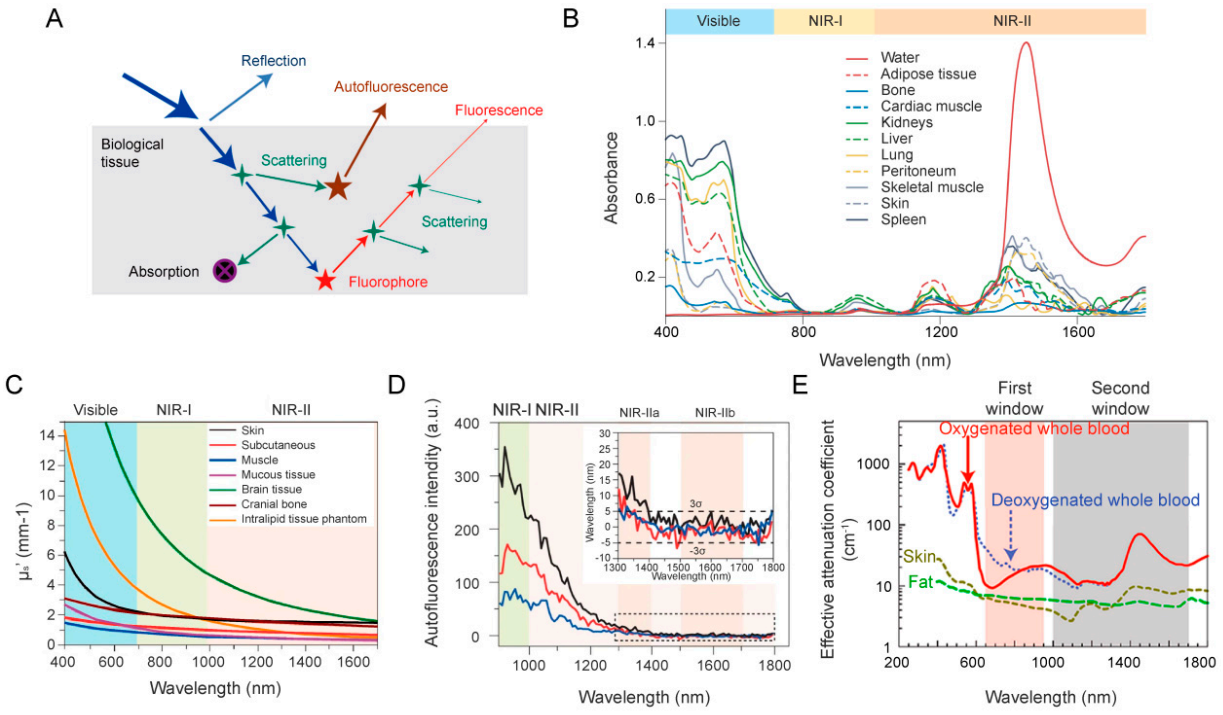

Figure 1. (**A**) Schematic diagram of the interactions between photons and tissue during fluorescence imaging. (**B**) Absorption spectra for water and various biological tissues in the visible and NIR window. (**C**) Reduced scattering coefficients among different biological tissues and intralipid solutions.

(**D**) Ex vivo autofluorescence spectra of mouse liver (black), spleen (red), and heart tissue (blue). (**E**) Effective attenuation coefficient of oxygenated blood, deoxygenated blood, skin, and fatty tissues. (**A**,**C**,**D**) reproduced with permission from [12], copyright 2017, Nature Publishing Group. (**B**) reproduced with permission from [13], copyright 2023, Nature Publishing Group. (**E**) reproduced with permission from [14], copyright 2009, Nature Publishing Group.

In this review, we aim to comprehensively elucidate the crucial role of NIR-II fluorescence imaging technology in precision nanomedicine delivery for cancer therapy. This review is structured into four main sections. Firstly, we discuss the existing physiological barriers encountered during nanomedicine delivery that hinder the delivery efficiency of nanomedicine to solid tumors. Secondly, we present the advantages and advancements of NIR-II fluorescence imaging technology, including imaging probes and imaging systems. Following this, we thoroughly explore the application of NIR-II fluorescence imaging technology in monitoring and evaluating various stages of nanomedicine delivery, including blood circulation, tumor accumulation, deep-tumor tissue penetration, cellular uptake, intracellular release, and therapeutic assessment. Finally, we elucidate the challenges and prospects of advanced NIR-II fluorescence imaging technology for precise nanomedicine delivery in cancer therapy (Figure 2).

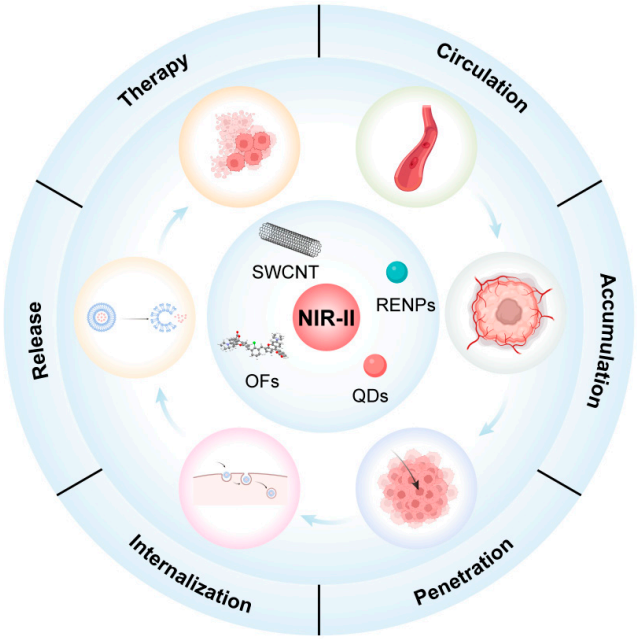

Figure 2. Illustrating advanced NIR-II fluorescence imaging technology for precise nanomedicine delivery in cancer therapy.

2. The Biological Barriers during the Nanomedicine Delivery Process

Despite the potential benefits of nanomedicines, their therapeutic efficacy for tumors is far from optimal. Wilhelm et al. conducted a study using a non-physiologically-based modeling approach based on published data from 2005 to 2015 and found that the mean and median delivery efficiencies were only 1.48% and 0.70% of the injected dose (%ID), respectively [15]. In contrast, Cheng et al. used physiologically-based pharmacokinetic (PBPK) models to analyze 376 datasets covering a wide range of nanomedicines published from 2005 to 2018, finding mean and median delivery efficiencies at the last sampling time point to be 2.23% and 0.76% ID, respectively [16]. Barriers include blood clearance, tumor accumulation, deep penetration, cellular internalization, and drug release (Figure 3) [17]. The entrapment of most nanomedicines in non-tumor tissue results in an inadequate drug dose reaching the lesion site. Addressing these barriers is crucial to improving the efficiency of nanomedicines in cancer therapy.

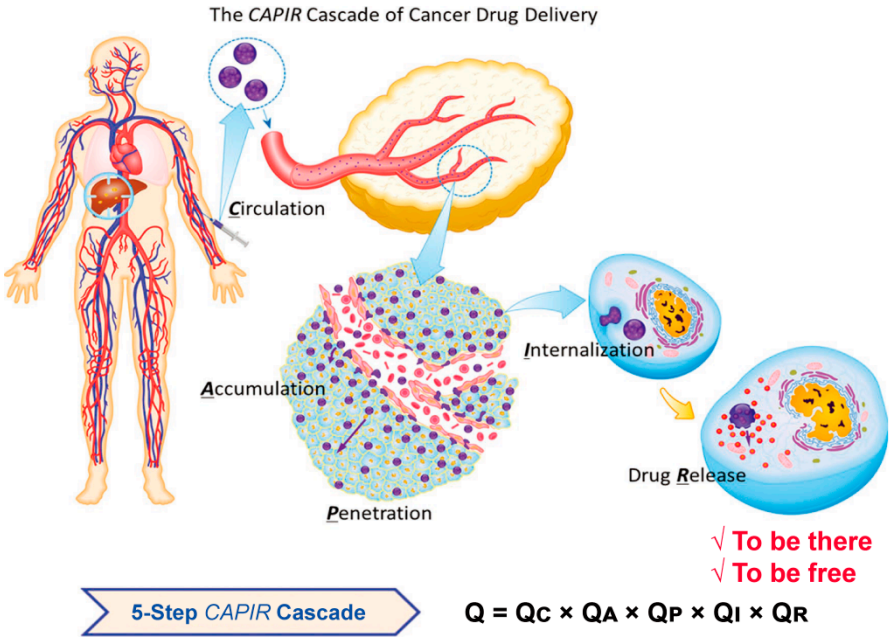

Figure 3. The CAPIR (**C**irculation, **A**ccumulation, **P**enetration, **I**nternalization, and **R**elease) cascade of the nanomedicine delivery system. The overall efficiency Q is the product of the efficiency of each step. Reproduced with permission from [17], copyright 2017, Wiley-VCH.

2.1. Blood Clearance

Rapid blood clearance is the first challenge that nanomedicines encounter upon entering the bloodstream [18,19]. In general, several inherent properties of nanomedicines are responsible for their clearance rates, such as their stability, size, shape, and surface chemistry properties [20,21]. The stability of nanomedicines determines whether they are prematurely released into the blood [22]. Nanomedicines smaller than 10 nm can be easily eliminated by passing through gaps in the healthy vessel endothelium. While larger spherical nanomedicines exhibit enhanced interaction with endothelial cells because they can sustain higher hemodynamic stresses and are closer to the vessel walls. Nanomedicines larger than 200 nm are prone to being taken up by the mononuclear phagocytic system (MPS), whereas those between 100 and 200 nm demonstrate prolonged circulation times [23]. In physiological environments, positively charged nanomedicines tend to interact more with negatively charged endothelial cell membranes, resulting in higher clearance rates. Negatively charged nanomedicines may bind to specific positively charged sites on the vessel walls, potentially shortening their circulation time in vivo. In contrast, neutral nanomedicines prevent interaction with the vessel walls, thereby extending circulation times [24,25]. Additionally, the configuration and composition of nanomedicine carriers play a significant role in determining their behavior within the bloodstream, including their mobility and the adsorption of various protein coronas. These factors, in turn, affect the overall transport and distribution of nanomedicines in the body [26].

2.2. Tumor Accumulation

Prolonging the blood circulation time of nanomedicine is fundamental for their accumulation in tumors [27]. The breakthrough of tumor blood vessels is the most critical step in achieving effective nanomedicine accumulation in tumors [28]. The abnormal structure and function of tumor blood vessels lead to poor vascular perfusion, which is an important obstacle to the accurate delivery of nanomedicine [29]. Although the exact mechanism of the enhanced permeability and retention (EPR) effect and the exact mechanism of the infiltration and accumulation of nanomaterials through tumor vessels in tumor stroma are still debated, recent studies have shown that passive exosmosis dominates in the vascular system of hyperpermeable tumors, while transendothelial transport is the main mechanism

in the vascular system of low-permeability tumors [30]. Furthermore, newly demonstrated basement membrane barriers can trap nanomedicine around tumor blood vessels, preventing its entry into the tumor tissue. Disrupting the basement membrane barrier can increase the extravasation of nanomedicine into the tumor stroma [31]. Another important strategy involves enhancing blood perfusion through various mechanisms and improving hypoxia to achieve normalization of the tumor vascular system [32].

2.3. Intratumoral Penetration

Upon accumulation at tumor sites, nanomedicines must navigate through tumor tissue via a series of interstitial pathways to exert their therapeutic effects on tumor cells [33]. However, the diffusion or penetration of nanomedicines at tumor sites is exceedingly challenging due to the unique microenvironment of tumors, such as abnormal vascular structures, a dense extracellular matrix, and elevated interstitial pressure [15]. The low concentration of the drug within tumor tissue may fail to eliminate all tumor cells, leading to tumor drug resistance and recurrence [34]. Thus, it is crucial to improve the penetration of nanomedicines into deep-tumor tissues for enhanced treatment outcomes [35]. During the penetration process, the size, shape, charge, and targeting modifications of nanomedicine may affect their diffusion rate, thereby affecting their penetration capability [36].

2.4. Cellular Internalization

The therapeutic targets of most drugs are located inside tumor cells; thus, their therapeutic efficacy largely relies on their ability to target intracellular components, emphasizing the importance of the efficient cellular uptake of drugs. However, nanomedicine with prolonged residence time in the bloodstream often conceals their surfaces, hindering their interactions with cancer cells and further inhibiting cell uptake [37]. Additionally, it is worth noting that cellular-level studies in vitro may not accurately reflect the complex interactions occurring at the nano-bio interface in vivo. Therefore, novel methods enabling the in situ observation of interactions between nanomedicine and target cells are needed to provide a more accurate understanding of their behavior and facilitate the development of improved drug delivery strategies.

2.5. Intracellular Drug Release

Traditional drug delivery often concludes with cellular uptake, but this may fall short of achieving the desired therapeutic effects due to rapid degradation within the harsh lysosomal environment—characterized by an acidic pH (4.5 to 5), high ionic strength, and a plethora of degradative enzymes—and the random distribution of drugs within the cell [38]. Eukaryotic organisms are distinguished by their membrane compartmentalization, which segregates various biochemical reactions into specific organelles or subcellular structures, essential for normal cellular functions. Precise subcellular nanomedicine delivery at the subcellular level is necessary to optimize therapeutic efficacy while minimizing dosage and side effects [39]. Therefore, lysosomal degradation and organelle membranes represent significant subcellular barriers to drug delivery. Additionally, the controlled release of multiple therapeutic agents is a critical advantage of nanomedicine, which is vital for achieving optimal outcomes and is not directly related to the amount of payload [40]. Moreover, the efflux of nanomedicine from tumor cells can also impact treatment results [41]. Consequently, achieving accurate subcellular targeting and controlled drug release behavior is crucial for enhancing clinical outcomes in cancer therapy.

Imaging technologies play a central role in elucidating the transport pathways of nanomedicines within the body and their interactions with tumors and other tissues, providing visualization strategies, especially for overcoming biological barriers [42]. A multitude of imaging techniques have been applied in the field of cancer therapy, enabling detailed pharmacokinetic and pharmacodynamic analyses of nanomaterials across various temporal and spatial scales [43]. The application of these technologies helps to precisely control the delivery process of nanomedicines, thereby enhancing therapeutic outcomes [44].

With advanced imaging methods, we can more accurately monitor the distribution and accumulation of nanomedicines within living organisms and their dynamic interactions with biological barriers, which is significant for optimizing cancer treatment strategies [45].

3. NIR-II Fluorescence Imaging Technologies

As a novel transparency window for biological tissue, NIR-II (1000–1700 nm) offers a penetration depth at the centimeter level, garnering significant interest in the realms of chemistry, materials science, and biology. Compared to the visible spectrum (400–650 nm) and NIR-I (650–950 nm), which have a penetration depth of only several millimeters, the NIR-II region benefits from reduced photon scattering and decreased tissue autofluorescence [46]. These advantages make it an indispensable tool for high-clarity, deep-tissue imaging, crucial for monitoring and assessing the fate of nanomedicines [47,48].

3.1. NIR-II Imaging Probes

Up to now, a series of high-performance NIR-II fluorescent probes have been developed both domestically and internationally, enabling high signal-to-noise ratio and high spatiotemporal resolution for in vivo imaging.

The trail was blazed in 2009 by Dai et al., who utilized single-walled carbon nanotubes (SWCNTs) for real-time in vivo imaging in the NIR-II window, exploiting their attributes for exceptional deep tissue penetration while minimizing autofluorescence [49,50]. Despite the breakthrough, the SWCNTs' quantum yield (QY) was relatively modest at 0.4% in the 1000–1300 nm range. This spurred further research geared toward enhancing their efficiency and expanding their emission wavelength into the NIR-IIb region (1500–1700 nm) by adjusting their dimensions [49,51].

Quantum dots (QDs) are another pivotal contributor to NIR-II imaging on account of their wide Stoke's shift, high photoluminescence QY, and precise emission spectra [52,53]. Nevertheless, their inherent toxicity casts a shadow over their use in live imaging [54]. In a crucial advancement, Wang et al. introduced the first heavy metal-free, biocompatible QDs made of Ag_2S with NIR-II emission, paving the way for their cellular and in vivo imaging applications [55–57]. Since then, a suite of QDs have entered the stage, showing promise as NIR-II imaging agents [58–62].

Additionally, rare-earth nanoparticles (RENPs) have taken a central role in NIR-II bioimaging [63]. Their narrow-band emissions, large Stoke's shift, and robustness make them suitable for a gamut of visualization applications [64]. Furthermore, adjusting factors like dopant levels, shell thickness, and crystal structure can substantially modify the fluorescence lifetimes of Ln^{3+} activators within RENPs, enriching the palette of NIR-II fluorescence properties and propelling the field of high-precision bioimaging forward [65–68].

Turning to the organic arena, NIR-II organic fluorophores are gaining recognition for in vivo imaging due to their excellent compatibility and pharmacokinetics [69]. With thoughtfully designed molecular structures, these fluorescent dyes boast high extinction coefficients and QYs. Furthermore, they excel in providing high-contrast images and superior resolution and can target specific biomarkers by altering their structure [70]. Such organic probes can also integrate functionalities like photothermal therapy and photoacoustic imaging by incorporating specific groups or nanoparticles [71].

While various types of NIR-II image probes have been developed, they still face several challenges, such as optical performance modulation through molecular structure design, doping system design, organic molecule water solubility issues, and safety concerns that require further assessment [72,73]. Despite these challenges, NIR-II imaging probes remain valuable tools for monitoring the behavior of nanomedicines in vivo. The fusion of nanomedicine with NIR-II fluorophores stands at the forefront of current research, utilizing innovative signal models that adjust in response to stimuli. This duality enables the precise tracking of nanomedicine delivery and the assessment of therapeutic outcomes, marking a significant advancement in realizing the potential of NIR-II for future medical imaging and therapy [74].

3.2. NIR-II Fluorescence Imaging Systems

In parallel with the development of NIR-II fluorophores, advancements in imaging systems are also highly important. The initial NIR-II fluorescence imaging system was based on InGaAs camera pairing with a macroscopic imaging lens, enabling the study of in vivo nanomedicine delivery in small animals at a macroscopic level [50,59]. As research requirements evolved, a diverse array of NIR-II imaging systems emerged. The wideband multiplexed in vivo imaging system, operating in the 400–1700 nm range, enabled real-time multi-channel imaging of NIR-II fluorescence and traditional fluorescence (visible and NIR-I fluorescence) through fluorescence coupling, catering to demands for the simultaneous imaging of various types of mixed drugs in small animals [75,76].

Various imaging instruments such as the NIR-II widefield microscope and wideband multiplexed microscope cater to in vivo studies on nanomedicine delivery at microscopic levels, including cells and microvessels [77–79]. Moreover, the development of NIR-II confocal and light-sheet microscopes enables 3D imaging at the microscopic scale [80–82]. A macroscopic NIR-II light-sheet imaging system has also been recently introduced for large-scale in vivo 3D imaging [83,84].

Notably, imaging instruments not only distinguish fluorescence intensity and fluorescence wavelength but also the differentiation of NIR-II imaging fluorophores in the temporal dimension through the development of NIR-II time-resolved in vivo imaging systems, providing a new approach to the analysis of multi-component mixtures [65]. With the continuous innovation of novel NIR-II fluorophores and imaging systems, NIR-II fluorescence imaging technology has become a powerful tool for precise nanomedicine delivery.

4. NIR-II Fluorescence Imaging for the Precise Evaluation of Nanomedicine Delivery in Cancer Therapy

4.1. Evaluation of Blood Circulation

In addition to factors such as particle size and morphology, the surface chemical properties of nanomedicines play a critical role in improving their circulation in the bloodstream. Two common methods are employed for this purpose. The first method is to modify the surface of nanomedicine with high biocompatibility polymer molecules such as polyethylene glycol (PEG). This modification helps prevent the absorption of plasma proteins and the clearance of nanomedicine by MPS [85]. The second method involves coating nanomedicine with membranes derived from red blood cells, platelets, stem cells, or immune cells, capitalizing on their high biocompatibility, low immunogenicity, and biological activity to achieve prolonged circulation [86]. Based on the advantages of fluorescence imaging in the NIR-II window, intuitive and visual in vivo imaging evidence is provided, indicating the distribution and pharmacokinetic characteristics of nanomedicine without the need for sacrificing animals for analysis at different time points [87].

For instance, Li et al. showcased a method for monitoring protein nanocages (PNCs) in living organisms using NIR-II Ag_2S QDs. By encapsulating these QDs within simian virus 40 (SV40) PNCs (PNC_{SV40}) and employing NIR-II imaging, they tracked PNC_{SV40} dynamics in mice with high precision. PEGylation strategies further revealed surface chemistry-dependent behaviors of PNC_{SV40} in vivo (Figure 4A) [87]. Xiao et al. developed a novel NIR-II fluorescent probe, L6-PEG_{2k}, which is based on a thiophenthiadiazole (TTD)-derived fluorophore and undergoes PEGylation to achieve prolonged circulation time in the body and efficient tumor-targeting imaging [88]. Additionally, Li et al. synthesized a D-A-D conjugated oligomer (DTTB) and utilized its NIR-II fluorescence emission properties to explore the impact of different chain lengths of PEG ligands on the nanomedicine's blood circulation half-life, presenting a promising real-time in vivo evaluation method for nanomedicine (Figure 4B) [89]. Moreover, Ding et al. employed semiconductor polymer nanoparticles (SPNs) as NIR-II fluorescence imaging agents to validate red blood cell membrane coatings to prolong blood circulation, subsequently reducing MPS uptake, facilitating the EPR effect, thus augmenting their accumulation in tumors (Figure 4C) [90].

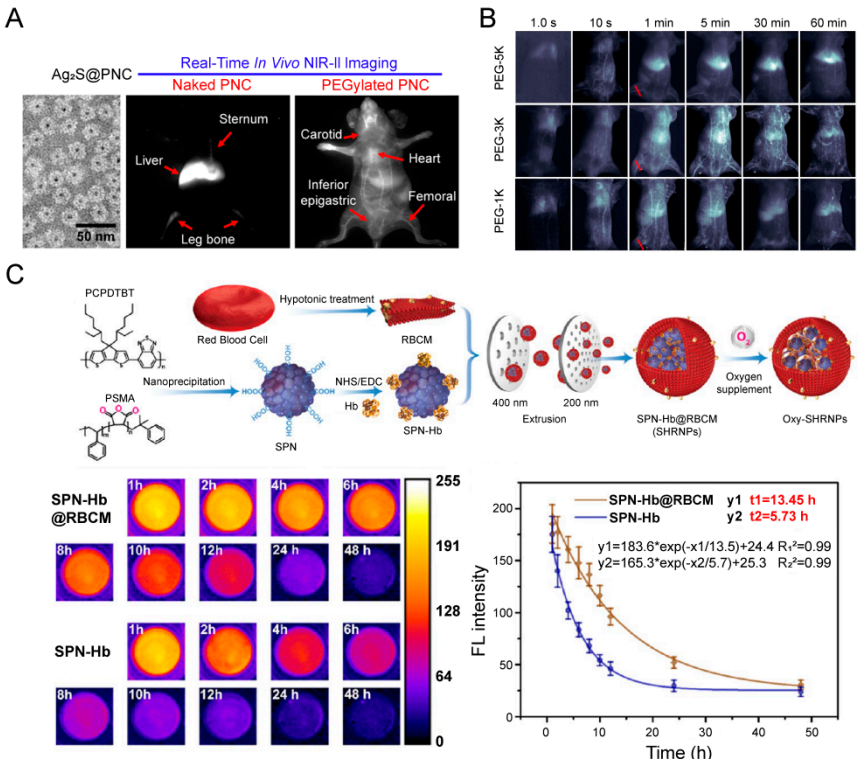

Figure 4. (**A**) The behaviors of protein nanocages in vivo, which are dependent on surface chemistry properties, can be monitored in real-time by encapsulating NIR-II Ag_2S QDs. Reproduced with permission from [87], copyright 2015, American Chemical Society. (**B**) A real-time evaluation of the pharmaceutical behavior of PEGylated nanomedicine using NIR-II fluorescence imaging in vivo. Red line: Fluorescence intensity measured along the red line. Reproduced with permission from [89], copyright 2020, American Chemical Society. (**C**) Synergetic chemo-photodynamic therapy against hypoxic tumors based on engineered red blood cell biomimetic nanovesicles with oxygen self-supply. Reproduced with permission from [90], copyright 2021, American Chemical Society.

4.2. Evaluation of Tumor Accumulation

Following the achievement of prolonged blood circulation, the subsequent crucial step in nanomedicine delivery involves facilitating the penetration of tumor vasculature through processes like extravasation or transcytosis and prolonging their residence time within the tumor microenvironment (TME). By doing so, it is possible to significantly enhance the accumulation of nanomedicine within the tumor, thereby potentially improving its therapeutic efficacy [91].

By modifying nanomedicine with ligands, such as antibodies, peptides, nucleic acid aptamers, folate (FA), etc., their adherence to tumor tissues and cell surfaces is enhanced, facilitating their selective delivery to tumors [92–94]. Song et al. proposed a novel nanomedicine (T&D@RGD-Ag_2S) that can rapidly and specifically bind to the tumor vasculature upon intravenous injection based on highly specific recognition between RGD peptide and integrin $\alpha_v\beta_3$. This targeting enhances tumor accumulation and improves tumor-to-background ratios (TBRs), observed through NIR-II fluorescence imaging. Additionally, the nanomedicine facilitates increased DOX delivery into tumors, leading to significant tumor cell apoptosis and marked tumor growth inhibition in a human U87-MG malignant glioma xenograft model (Figure 5A) [95]. Wang et al. introduced TPE-BT-BBTD, a 980 nm absorbing agent ideal for deep-seated tumor treatment. This compound excels in deep NIR-II fluorescence imaging and potent photothermal performance, crucial for advanced pancreatic cancer therapy. When coupling it with αPD-L1 antibodies, αPD-L1@TPE-BT-BBTD nanoparticles offer precise tumor targeting and robust reversal of immunosuppression [96]. Additionally, Liu et al. developed BDP-T-N-DTX-FA, encapsulating the chemotherapeutic drug docetaxel

(DTX) within thiophene-based boron dipyrromethene (BDP) nanoparticles. These nanoparticles demonstrated high signal-to-background ratios of up to 11.8 in tumor accumulation (Figure 5B) [97].

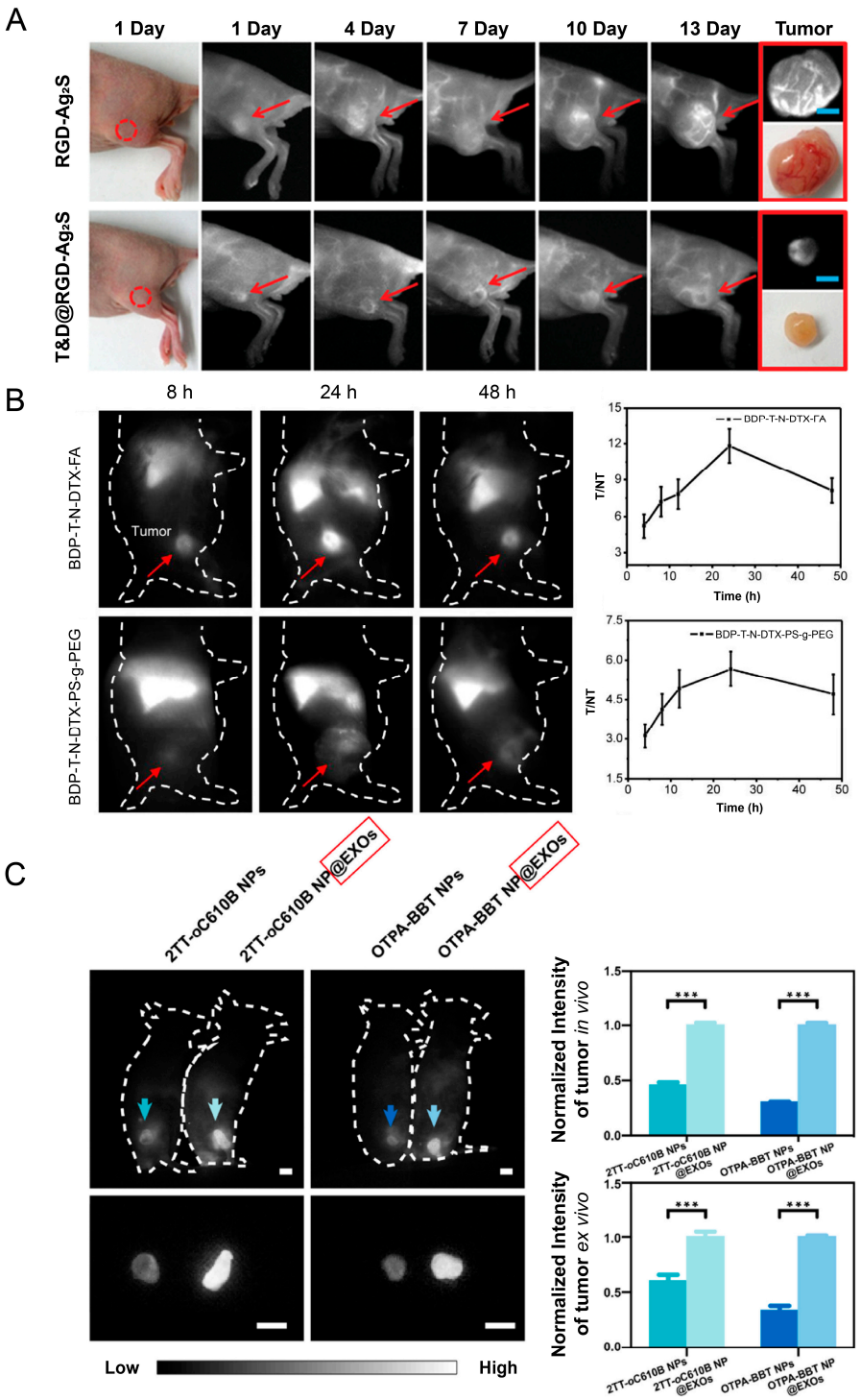

Figure 5. (**A**) In vivo real-time visualization of tumor angiogenesis. Scale bar: 0.5 cm. Reproduced with permission from [95], copyright 2016, Wiley-VCH. (**B**) In vivo fluorescence imaging in the NIR-IIb window and biodistribution of BDP-T-N-DTX-FA and BDP-T-N-DTX-PS-g-PEG. Reproduced with permission from [97], copyright 2021, Elsevier Ltd. (**C**) Verification of EXO in bio-excretable AIE materials. Scale bar: 5 mm (n = 3, *** $p < 0.001$). Reproduced with permission from [98], copyright 2021, Elsevier Ltd.

Research indicates that cancer cell membranes contain numerous transmembrane proteins like CD47 that can inhibit macrophage phagocytosis and the targeting properties of adhesive factors [99]. Modifying cancer cell membranes onto the surface of nanomaterial not only prolongs their circulation time but also imparts homologous targeting properties to them [100,101]. Zhang et al. confirmed that tumor cell membrane-coated nanomedicine shows increased tumor accumulation compared to PEGylated RENP via NIR-II fluorescence imaging. A significantly higher T/N was observed in tumor mice models injected with CC-Nd@PEG than those injected with Nd@PEG after 24 h [102]. Moreover, Zhang et al. showcased a significantly increased accumulation of nanomedicine in tumors using tumor cell membrane-modified Ag_2Te QDs through in vivo NIR-II fluorescence imaging. By leveraging the active homotypic tumor targeting ability inherent to the cell membrane and the passive enhanced permeation and retention effects, they achieved enhanced accumulation at tumor sites ((31 $\pm$ 2)% injection dose per gram of tumor) and a high tumor-to-normal tissue ratio (13.3 $\pm$ 0.7) [103]. Exosomes (EXOs), small vesicles released by cells during plasma membrane fusion, have been utilized in nanomedicine [104]. Li et al. prepared relatively larger electroporated exosome-hybridized nano-vesicles TT3-oCB NP@EXOs, confirming their specific targeting ability in vitro through aggregation-induced emission (AIE) in the NIR-II region and demonstrating their homologous tumor-targeting ability in vivo (Figure 5C) [98].

In addition, small, molecular, self-assembled nanoparticles can achieve enhanced tumor retention by leveraging the characteristics of the TME, such as pH. Chen et al. developed SIMM1000, a pH-sensitive dye for advanced NIR-II imaging, targeting tumors in animals. Leveraging RGD for targeting, the EPR effect, and pH-triggered assembly, it significantly boosts tumor accumulation and offers a much higher tumor-to-normal tissue ratio (~10) than traditional NIR-I agents (~3) [105]. Li et al. developed a pH-sensitive self-assembling peptide dye CR-PEG-GBP for NIR-II imaging and guided therapy applications. This nanoprobe selectively aggregates within the tumor microenvironment, allowing for higher tumor accumulation and longer retention times, without causing harm to normal tissue. It shows potential for imaging-guided photothermal therapy and sonodynamic therapy in treating HCC [106].

4.3. Evaluation of Tumor Tissue Penetration

The highly dense tumor extracellular matrix (ECM) within tumors poses a formidable obstacle to effective drug penetration into tumor tissues. Currently, research on nanomedicine penetration into tumors remains relatively limited. To validate the effectiveness of deep stromal penetration strategies, the NIR-II fluorescence imaging technology offers substantial advantages in terms of high tissue penetration depth, spatiotemporal resolution, and sensitivity.

Strategies to enhance the penetration efficiency of nanomedicine in tumors typically involve the customization of nanomedicine properties and modulation of the TME [107]. Tailoring the size, shape, and surface chemical properties of nanomedicines is crucial for mitigating diffusion barriers [108]. In certain instances, ultra-small nanoparticles penetrate deeply into tumor tissues without necessitating modifications [109]. For instance, Han et al. developed ultra-small penetrable carbon dots (PCDs) with NIR-II fluorescence properties and validated their penetration capabilities within tumor spheroids and deep tissues using NIR-II fluorescence imaging (Figure 6A) [110].

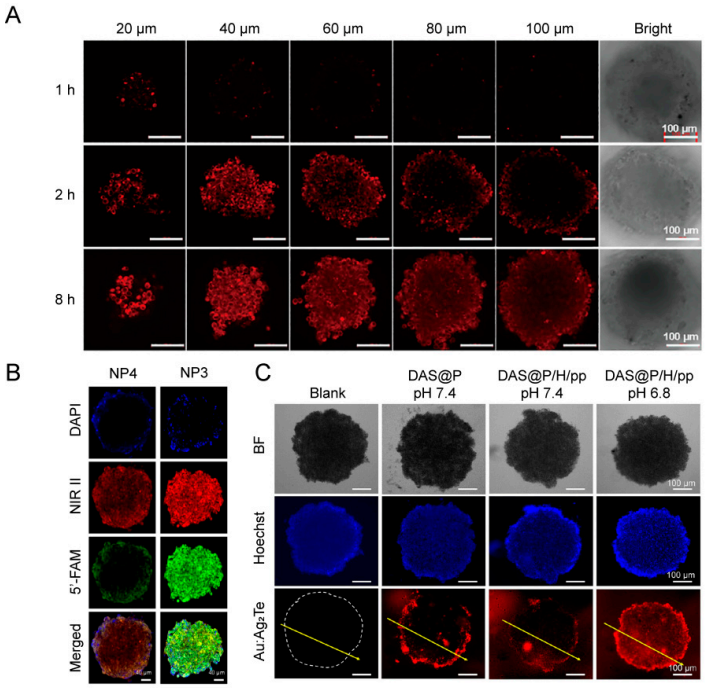

Figure 6. (**A**) Permeation of PCD in tumor spheres and solid tumors. Reproduced with permission from [110], copyright 2022, Elsevier Ltd. (**B**) Imaging simultaneous uptake of nanoparticles into 3D tumor spheres. Reproduced with permission from [111], copyright 2021, American Chemical Society. (**C**) Fluorescence microscopy observations of DAS@P/H/pp penetrating Panc-1tumorspheroids. Representative images of the distribution of DAS@P/H/pp in the middle layers of the spheroids under different pH conditions: nucleus (blue) and DAS@P/H/pp (red). Yellow arrow: Fluorescence signal intensity measured along the yellow arrows. Reproduced with permission from [112], copyright 2024, American Chemical Society.

Nanomedicine with a diameter of approximately 100 nm exhibits prolonged circulation time in the bloodstream but may encounter challenges in penetrating the core of tumors. Matrix-rich tumors typically restrict penetration to nanoparticles with a diameter < 50 nm [113]. Hence, developing size-transformable nanomedicine can address these conflicting requirements, representing a promising approach to reconciling these conflicting requirements [114]. By harnessing tandem NIR-II fluorophores, Wei et al. developed biodegradable polyester nanoparticles. The nanoparticles incorporated a platinum intercalator (56MESS) and were conjugated with a cell-targeting RGD peptide and a caspase-3 cleavable peptide probe. Utilizing NIR-II imaging technology, it was observed that the nanoparticles successfully infiltrated 3D tumor spheroids (Figure 6B) [111].

The degradation of ECM or inhibition of ECM generation has been proven to enhance the diffusion of nanomedicine in solid tumors [115]. For example, enzymatic degradation of collagen within tumors, inhibiting collagen synthesis, reducing hyaluronic acid production, and alleviating solid stress, can improve the deep penetration of nanomedicine into tumors [116]. Exploiting the acidic nature of the tumor microenvironment, Yang et al. engineered a TME-responsive nanomedicine, DAS@P/H/pp, which facilitates the penetration and accumulation of NK92 cells within pancreatic cancer tumors. Upon encountering the acidic tumor milieu, DAS@P/H/pp undergoes a charge reversal and releases hyaluronidase (HAase), effectively degrading the extracellular matrix and enhancing drug delivery. The nanomedicine's performance, including its ability to guide NK92 cells into the tumor core, is monitored and visualized using multiplexed NIR-II fluorescence imaging, which provides a non-invasive means to assess tumor penetration and therapeutic efficacy (Figure 6C) [112]. A promising strategy for improving deep penetration and tumor targeting within ECM-rich tumor tissues involves pulsed, high-intensity, focused ultrasound to reshape ECM and disrupt collagen structures [117]. However, disrupting the TME might

increase the risk of tumor invasion and metastasis. Currently, there is a scarcity of research utilizing in vivo imaging to validate related strategies.

4.4. Evaluation of Cellular Internalization

Most drug targets are inside tumor cells; therefore, whether a drug achieves intracellular localization and specific target release is crucial for its therapeutic efficacy [118–121]. Several strategies involve using the tumor-specific microenvironment to trigger changes in the surface chemical properties of nanomedicines, such as charge conversion, ligand exposure, and hydrophobic alterations, enabling the nanomedicines to overcome the cell membrane barrier and effectively interact with cancer cells [120]. Antaris et al. demonstrated the robust molecular selectivity of CH1055-affibody toward EGFR+ cancer cells via in vitro NIR-II imaging (Figure 7A) [122]. Wang et al. reported the utilization of a conjugated NIR-II fluorescent probe targeting the tumor stem cell biomarker CD133 for molecular tumor imaging. HEK293T spots showed a much weaker NIR-II fluorescence intensity compared to U87MG spots, indicating a high affinity of the CP-conjugated NIR-II molecular probes for the specific recognition of CP-CD133. In vitro molecular imaging confirmed this result (Figure 7B) [123]. Wen et al. presented a straightforward approach to fabricate a novel, chain-like NIR-II nanoprobe (APP-Ag_2S-RGD) by employing self-assembly of an amphiphilic peptide (APP) into nanochains followed by the crosslinking of Ag_2S QDs and the targeted RGD. Using a fluorescence microscope, they demonstrated the effectiveness of APP-Ag_2S-RGD in targeting cancer cells (Figure 7C) [124]. Yuan et al. developed semiconductor polymer nanoparticles (SPN-PTs) based on oligopeptide PT, demonstrating their targeting capability for osteosarcoma. These nanoparticles are actively internalized into osteosarcomic cells, exhibiting faster uptake rates and excellent selectivity. Through NIR-II fluorescence and PA signals, these nanoparticles enable accurate early diagnosis of osteosarcoma and provide efficient PTT and photodynamic therapy (PDT) both in vitro and in vivo [125]. Zhang et al. designed a cascade-targeting NIR-II fluorescence nanoparticle (NPER/BO-PDT), initially targeting bone tumors and subsequently homing in on subcellular organelles within the endoplasmic reticulum (ER) [126]. He et al. crafted a CEAF probe comprising a hydrophilic polymer and an acid pH-sensitive fluorescent segment for NIR-II imaging. This probe remains quenched in water and blood but becomes activated upon cell endocytosis. The probe localizes lysosomes, offering specific signals for tumor and inflammation imaging with extended observation times (Figure 7D) [127].

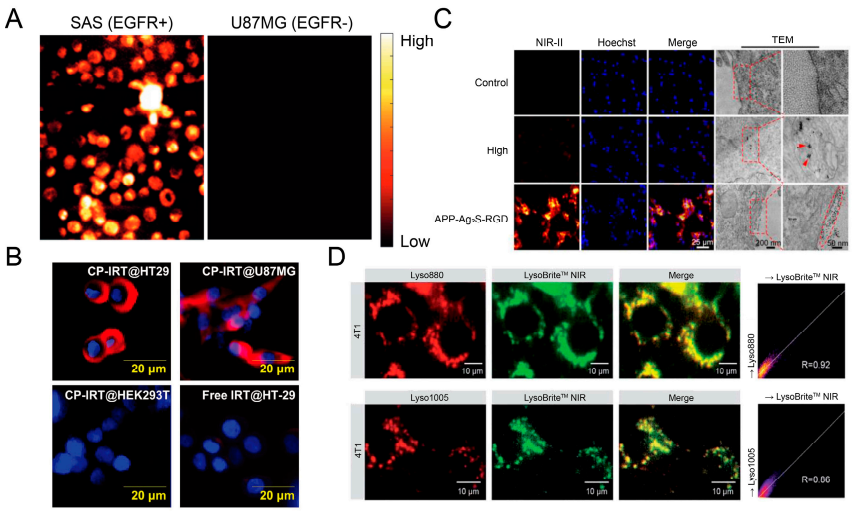

Figure 7. (**A**) Molecular imaging of cancer cells revealed robust selective staining in vitro for the squamous cell carcinoma (SAS) cell line, contrasting with the low EGFR levels observed in U87MG cells. Reproduced with permission from [122], copyright 2016, Springer Nature. (**B**) CP-IRT binding behavior toward HT-29 (CD133-positive), U87MG (CD133-positive), HEK293 (CD133-negative), and free dyes toward HT-29. Reproduced with permission from [123], copyright 2018, Wiley-VCH.

(**C**) TEM and fluorescence images of U87-MG cells incubated with Ag_2S-RGD or APP-Ag_2S-RGD (Ag_2S QD concentration 80 μg·mL^{-1}). Red arrows and dotted circles indicate Ag_2S QDs. Reproduced with permission from [124], copyright 2019, Wiley-VCH. (**D**) Epifluorescence images of 4T1 cells. Reproduced with permission from [127], copyright 2021, Royal Society of Chemistry.

4.5. Evaluation of Drug Release

Moreover, after nanomedicines are internalized by tumor cells, precise release at the target site is even more critical [128]. NIR-II fluorescence imaging is commonly employed to monitor drug release, often based on mechanisms such as competitive absorption (ACIE) and fluorescence resonance energy transfer (FRET), to precisely report drug release [129,130]. Nanocarriers possess characteristics that respond to the abnormal tumor microenvironment, such as low pH, high ROS, GSH, and enzymes, enabling controlled drug release [131].

Wang et al. presented a multi-excitable NIR biological imaging technique based on NIR-II DCNP with competitive absorption-induced emission. In vivo, drug release can be semi-quantitatively monitored by measuring the fluorescence signal in the NIR-II window of lanthanide-downconverted nanoparticles (Figure 8A) [132]. Leveraging the slight acidic property of tumors, Ling et al. developed a TME-responsive nanomedicine, FEAD1, which decomposes Fmoc-His metal coordinations and DOX hydrophobic interactions. As a result, Ag_2S NIR-II fluorescence is initiated due to the oxidation of A1094, illuminating the tumor tissues and facilitating the rapid release of DOX within the tumor, thereby resulting in precise tumor therapy (Figure 8B) [133]. Tang et al. reported a nanomedicine, NP@PEDOX/PSP, capable of effectively inducing ROS and facilitating rapid DOX release under 808 nm laser irradiation while also exhibiting intense NIR-II fluorescence (Figure 8C) [134]. Xie et al. developed an innovative nano-drug delivery system for NIR-II fluorescence imaging, enabling the real-time monitoring of drug release and targeted chemotherapy for cancer. The cumulative drug release showed a linear correlation with NIR-II fluorescence intensity [135]. Dai et al. devised a TME-responsive NIR-II phototheranostic nanoplatform AFD NPs based on FRET. These nanoparticles combine NIR-II Ag_2S QDs and NIR-II quencher DBZ Pdots with Fe(III) for assembly. Within the tumor environment, abundant GSH triggers a rapid "turn-on" of NIR-II fluorescence, achieving higher tumor-to-normal tissue signal ratios. Additionally, these nanoparticles enable NIR-II photothermal and chemodynamic therapies, leveraging GSH depletion and NIR-II PTT to enhance CDT-induced oxidative damage for a synergistic anti-tumor effect [136].

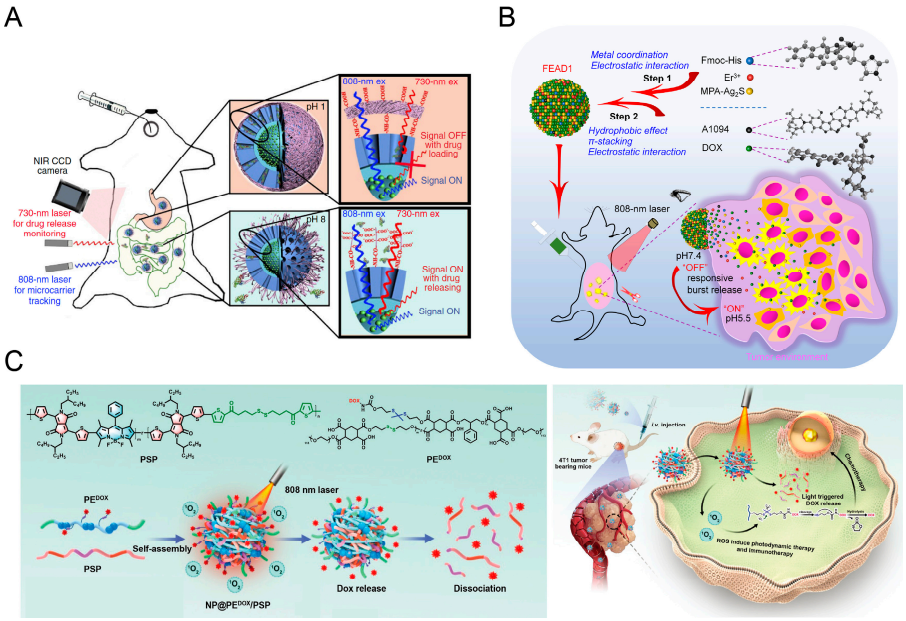

Figure 8. (**A**) Schematic illustration of the ACIE bioimaging system and fabrication procedure. Reproduced with permission from [132], copyright 2017, Springer Nature. (**B**) Illustration of the

functional NIR-II nanotheranostic system FEAD1, which is capable of diagnosing and treating peritoneal metastases with pinpoint accuracy. Reproduced with permission from [133], copyright 2020, Wiley-VCH. (**C**) Schematic illustration of the self-sacrificially degradable NIR-II theranostic NP@PEDOX/PSP for photodynamic immunotherapy. Reproduced with permission from [134], copyright 2022, Wiley-VCH.

4.6. Evaluation of Therapeutic Effects

NIR-II fluorescence imaging also serves as a valuable tool in the in vivo visualization approach to therapeutic efficacy assessment. Chen et al. developed a catalytic, microenvironment-tailored nanoreactor (CMTN) containing a MoO_4^{2-} catalyst and alkaline sodium carbonate. This CMTN provides an optimal pH environment for MoO_4^{2-}-catalyzed singlet oxygen ($^1O_2$) generation from H_2O_2 while protecting the catalyst from GSH chelation. The liposomal membrane allows H_2O_2 and $^1O_2$ to freely cross, enabling the CMTN to achieve monitored tumor photodynamic therapy with its NIR-II ratiometric fluorescent $^1O_2$ sensor [137]. Fu et al. developed a caspase-3-activated nanoprobe, AuNNP@DEVD-IR1048, for the early assessment of RT efficacy. This nanoprobe consists of nanogapped gold nanoparticles (AuNNPs) and NIR-II fluorescent molecules (IR-1048) linked by a caspase-3-specific peptide sequence (DEVD). Upon X-ray irradiation, caspase-3 is activated and the DEVD sequence is cleaved, activating NIR-II FL and PA imaging signals. NIR-II FL/PA signals exhibit a positive correlation with caspase-3 levels, while levels of activated caspase-3 inversely correlate with tumor size. The study demonstrates the potential of activated NIR-II FL/PA imaging for the timely prediction and evaluation of RT efficacy (Figure 9A) [138]. Su et al. developed an $^1O_2$-responsive theranostic platform based on thiophene-based small molecules (2SeFT-PEG) and chlorin e6 (Ce6) micelles. By monitoring changes in chemiluminescence (CL) and fluorescence (FL) signals at 1050 nm, the platform enables the real-time assessment of PDT efficacy. The ratiometric NIR-II CL/FL imaging accurately quantifies $^1O_2$ concentration and O_2 consumption or recovery, allowing for the evaluation of PDT therapeutic efficacy in vivo (Figure 9B) [139]. Yuan et al. developed a self-luminous small molecule (CLPD) for ratiometric bioluminescence (BL)/fluorescence (FL) imaging based on the bioluminescence resonance energy transfer (BRET) mechanism. The early assessment of PDT efficacy is provided by using CLPD for the NIR-II BL imaging of ROS generated during PDT. A reliable correlation between the ratiometric NIR-II BL/FL signal and tumor size is established, offering a reliable method for evaluating therapeutic outcomes (Figure 9C) [140].

4.7. Evaluation of Targeted Tumor Delivery

For brain tumors and bone-associated tumors, overcoming the blood–brain barrier (BBB) and blood-bone marrow barrier (BMB) is essential for effective nanomedicine delivery. NIR-II fluorescence imaging offers a valuable tool for visualizing the precise targeting and delivery process of nanomedicine.

Nanomedicine can cross the BBB and reach brain tumors through various physiological pathways, such as receptor-mediated transcytosis (RMT) and adsorption-mediated transcytosis (AMT) [141]. For example, Xiao et al. synthesized a DNA block copolymer PS-b-DNA that can traverse the BBB through SR-mediated transcytosis, facilitating targeted delivery to brain tumors. This process of targeting glioblastoma was visualized through NIR-II fluorescence imaging (Figure 10A) [142]. As well, Li et al. demonstrated the efficacy of Ag_2S QD-based nanomedicine in inhibiting osteolysis and chemotherapy in an orthotopic bone tumor model. The in vivo targeted delivery of DOX to the bone tumor was clearly observed leveraging the high spatiotemporal resolution of NIR-II fluorescence imaging (Figure 10B) [143].

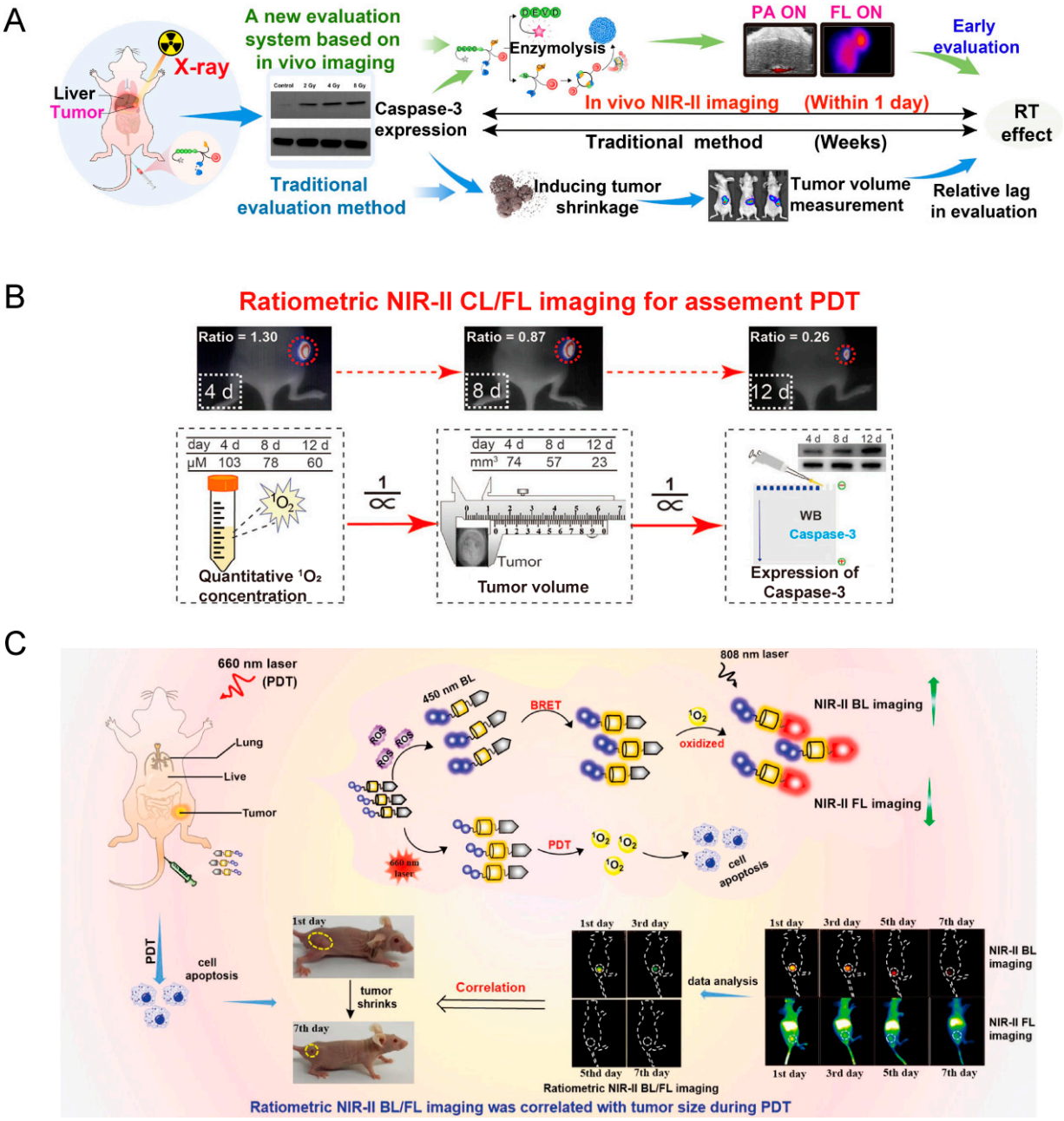

Figure 9. (**A**) Early prediction and real-time evaluation of RT effect using the caspase-3 enzyme-activatable AuNNP@DEVD-IR1048 nanoprobe in combination with NIR-II FL/PA bimodal imaging. Reproduced with permission from [138], copyright 2022, Wiley-VCH. (**B**) NIR-II CL and FL imaging for the assessment, planning, and monitoring of PDT. Reproduced with permission from [139], copyright 2022, Wiley-VCH. (**C**) In vivo NIR-II ratiometric BL and FL imaging using CLPD and early self-evaluation of PDT after cancer diagnosis. Reproduced with permission from [140], copyright 2023, Wiley-VCH.

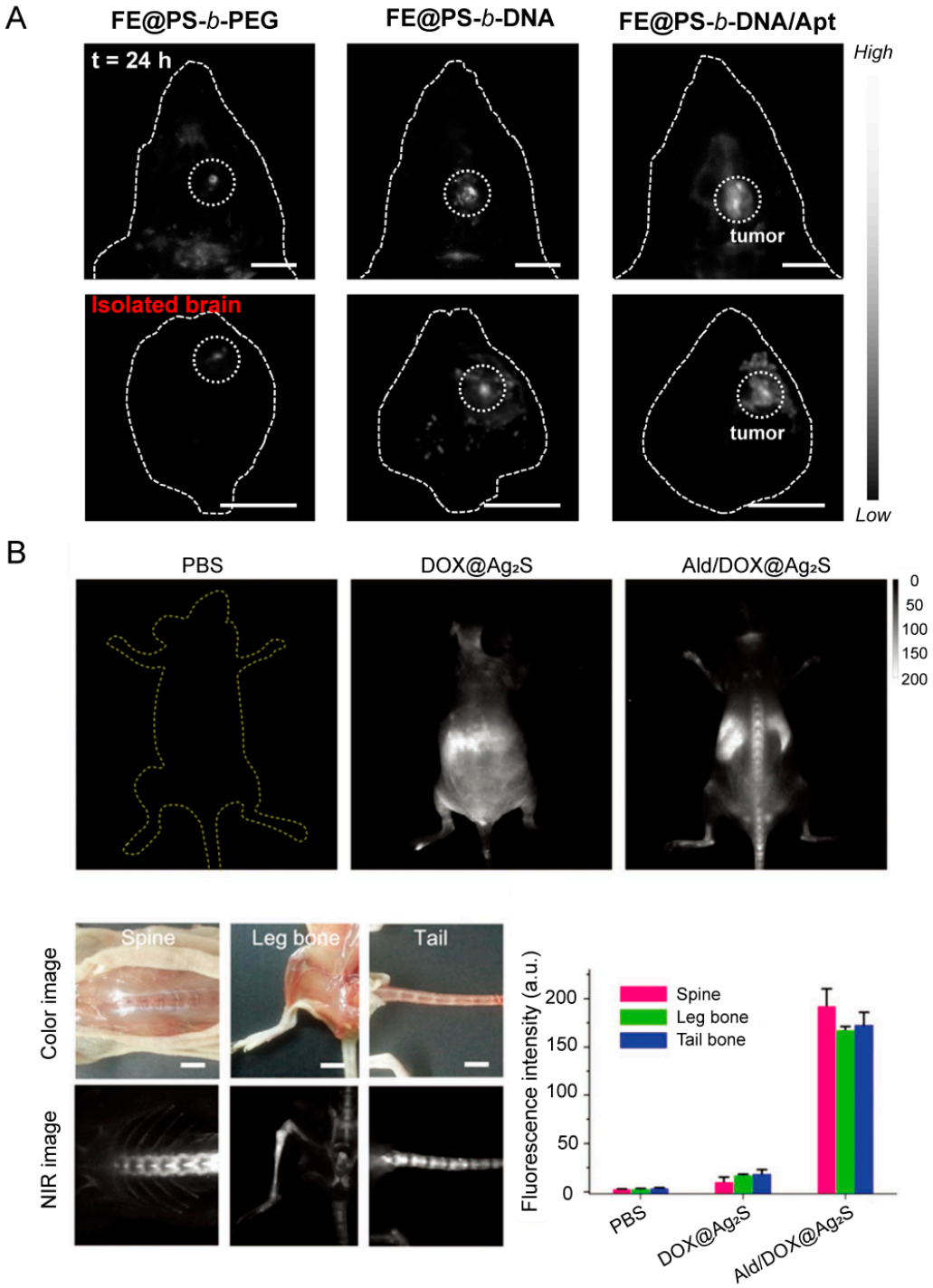

Figure 10. (**A**) Tracking the process of crossing the blood-brain barrier (BBB) and targeting glioblastoma through NIR-II fluorescence imaging. Reproduced with permission from [142], copyright 2020, Wiley-VCH. (**B**) NIR-II fluorescence images of living mice after intravenous injection of Ald/DOX@Ag_2S. Reproduced with permission from [143], copyright 2017, Wiley-VCH.

5. Conclusions and Outlook

NIR-II fluorescence imaging demonstrates great potential for monitoring nanomedicine delivery and assessing treatment outcomes for tumors due to its deep tissue penetration capability, high spatiotemporal resolution, and negligible autofluorescence, facilitating the precise design and guidance of nanomedicine. This review discussed the current progress of NIR-II imaging technology, including fluorophores and imaging systems. It also highlighted the challenges in achieving precise in vivo nanomedicine delivery, including

blood clearance, tumor accumulation, deep penetration, cellular internalization, and drug release. Based on NIR-II fluorescence imaging, five key processes alongside addressing BBB and BMB were emphasized for optimizing nanomedicine delivery systems. Moreover, this review highlighted the potential of NIR-II imaging as a tool for evaluating treatment effectiveness. Despite notable advancements in this field, there exists substantial scope for further expansion and optimization.

In the development of NIR-II imaging fluorophores, it is critical to improve both the optical performance of the probes and the safety and reliability of their labeling techniques. Firstly, optical performance is foundational for efficient NIR-II imaging, encompassing the selection of the correct wavelength range, ensuring a high QY, and maintaining stable emission. Probes in the NIR-IIb spectrum (1500–1700 nm) are preferred for their reduced light scattering and enhanced tissue penetration. A high QY amplifies imaging sensitivity by emitting stronger signals upon given light excitation, while a stable emission pattern keeps the signal consistency high, improving image precision. Beyond fluorescence, exploring the lifetime, Raman, and photoacoustic properties of the fluorescence groups can broaden the application of NIR-II optical imaging in nanomedicine research. Secondly, the labeling techniques for these probes must be safe, non or minimally interfering, and stable. Safety ensures that the probes are non-toxic and free from side effects in a biological environment; it also ensures that the introduction of probes does not impair the original functions and efficacy of nanomedicines. For nanoliposome drugs, developing membrane-embedded probes for their labeling and tracking is an optional strategy. Additionally, based on bio-orthogonal click reactions, it is possible to achieve the site-specific, long-term, stable labeling of drugs. Thirdly, developing probes that respond to different physiological and pathological microenvironments is essential for assessing the precision of nanomedicine delivery and evaluating therapeutic outcomes. Developing various response modes such as quenching, activation, and ratio modes, along with other response modes that include changes in fluorescence lifetime and fluorescence anisotropy, allows for the qualitative and quantitative analysis of nanomedicine administration processes in vivo. The coordination of these factors significantly enhances the role of NIR-II optical imaging in cancer diagnosis and treatment, markedly improving the accuracy and specificity of nanomedicine delivery.

The continuous innovation of NIR-II imaging systems will be key to deepening our understanding of nanomedicine, advancing personalized clinical treatments, and accurately predicting patient outcomes. Firstly, from administration to reaching their target, nanomedicines must navigate transitions across whole-body, organ, tissue, cell, and molecular dimensions. To comprehensively understand their pharmacokinetics and pharmacodynamics in vivo, developing cross-scale, in situ, real-time live imaging techniques is essential. Secondly, as the current imaging paradigms are primarily two-dimensional, developing three-dimensional, quantifiable imaging systems, such as rapid NIR-II light sheet imaging systems, is critical for advancing nanomedicine research. Thirdly, given the significant heterogeneity of tumors, optical imaging, while offering a channel for functional imaging data, often fails to provide a complete view of nanomedicines in vivo when used alone. Therefore, the integration of structural imaging techniques, including Raman, X-ray, CT, and MRI, among others, is necessary.

Given the heterogeneity of tumor structure and function, the complexity of nanomedicine interactions at the tumor interface, and the dynamic spatiotemporal evolution of the tumor microenvironment, it becomes crucial to combine long-term monitoring, a multiscale viewpoint, and a systematic analysis of multisource data. In this vein, leveraging artificial intelligence (AI) is indispensable for enhancing the quality and interpretability of NIR-II multimodal imaging data. First, by applying AI to data preprocessing, including denoising and enhancing imaging data, significant improvements in imaging quality and clearer visual representation are achieved. Second, AI-driven data mining and analysis aid in extracting key patterns and features from voluminous imaging datasets, thus achieving precise localization in nanomedicine. This precise localization assists in selecting the most effective nanomedicine delivery systems. This comprehensive approach ensures a

systematic assessment of the complex interactions within the tumor microenvironment, supporting the ongoing refinement and optimization of nanomedicine delivery methods.

In conclusion, further investigations are warranted to overcome the current obstacles. Leveraging the potential of NIR-II optical imaging in guiding the design of anti-tumor nanomedicine delivery systems will significantly contribute to new drug development and clinical therapy.

Author Contributions: M.L. contributed to writing the original manuscript. M.L., T.L., F.W., F.R., S.X. and C.L. revised the manuscript. All authors have read and agreed to the published version of the manuscript.

Funding: This work was supported by the National Key Research and Development Program of China (grant no. 2021YFF0701804), the National Natural Science Foundation of China (grant nos. 22174158, 22104150, and 22201297), the Science and Technology Project of Suzhou (grant no. SJC2022001), and the Natural Science Foundation of Jiangsu Province (grant nos. BK20232046 and BK20210128).

Institutional Review Board Statement: Not applicable.

Informed Consent Statement: Not applicable.

Data Availability Statement: There were no new data created or analyzed in this study. Data sharing does not apply to this article.

Conflicts of Interest: The authors declare no conflicts of interest.

References

1. Sung, H.; Ferlay, J.; Siegel, R.L.; Laversanne, M.; Soerjomataram, I.; Jemal, A.; Bray, F. Global Cancer Statistics 2020: GLOBOCAN Estimates of Incidence and Mortality Worldwide for 36 Cancers in 185 Countries. *CA Cancer J. Clin.* **2021**, *71*, 209–249. [CrossRef] [PubMed]
2. Xia, C.; Basu, P.; Kramer, B.S.; Li, H.; Qu, C.; Yu, X.Q.; Canfell, K.; Qiao, Y.; Armstrong, B.K.; Chen, W. Cancer Screening in China: A Steep Road from Evidence to Implementation. *Lancet Public Health* **2023**, *8*, e996–e1005. [CrossRef] [PubMed]
3. Siegel, R.L.; Miller, K.D.; Wagle, N.S.; Jemal, A. Cancer Statistics, 2023. *CA Cancer J. Clin.* **2023**, *73*, 17–48. [CrossRef] [PubMed]
4. Chan, W.C.W. Principles of Nanoparticle Delivery to Solid Tumors. *BME Front.* **2023**, *4*, 0016. [CrossRef] [PubMed]
5. Li, R.; Bao, Z.; Wang, P.; Deng, Y.; Fan, J.; Zhu, X.; Xia, X.; Song, Y.; Yao, H.; Li, D. Gelatin-Functionalized Carbon Nanotubes Loaded with Cisplatin for Anti-Cancer Therapy. *Polymers* **2023**, *15*, 3333. [CrossRef] [PubMed]
6. Lammers, T. Nanomedicine Tumor Targeting. *Adv. Mater.* **2024**, 2312169. [CrossRef]
7. Ta, W.; Li, X.; Song, J.; Hua, R.; Zheng, Y.; Lu, W. Customizable Dual-Fluorescent Nanoparticles for Tracing and Quantifying of Cell Transport. *Int. J. Nanomed.* **2023**, *18*, 1823–1834. [CrossRef] [PubMed]
8. Cook, A.B.; Decuzzi, P. Harnessing Endogenous Stimuli for Responsive Materials in Theranostics. *ACS Nano* **2021**, *15*, 2068–2098. [CrossRef] [PubMed]
9. Xu, Z.; Qian, J.; Meng, C.; Liu, Y.; Ding, Q.; Wu, H.; Li, P.; Ran, F.; Liu, G.-Q.; Wang, Y.; et al. TME-Targeting Theranostic Agent Uses NIR Tracking for Tumor Diagnosis and Surgical Resection and Acts as Chemotherapeutic Showing Enhanced Efficiency and Minimal Toxicity. *Theranostics* **2022**, *12*, 2535–2548. [CrossRef]
10. Zhang, K.; Chen, F.-R.; Wang, L.; Hu, J. Second Near-Infrared (NIR-II) Window for Imaging-Navigated Modulation of Brain Structure and Function. *Small* **2023**, *19*, 2206044. [CrossRef]
11. Meng, X.; Pang, X.; Zhang, K.; Gong, C.; Yang, J.; Dong, H.; Zhang, X. Recent Advances in Near-Infrared-II Fluorescence Imaging for Deep-Tissue Molecular Analysis and Cancer Diagnosis. *Small* **2022**, *18*, 2202035. [CrossRef] [PubMed]
12. Hong, G.; Antaris, A.L.; Dai, H. Near-Infrared Fluorophores for Biomedical Imaging. *Nat. Biomed. Eng.* **2017**, *1*, 0010. [CrossRef]
13. Chen, Y.; Wang, S.; Zhang, F. Near-Infrared Luminescence High-Contrast in Vivo Biomedical Imaging. *Nat. Rev. Bioeng.* **2023**, *1*, 60–78. [CrossRef]
14. Smith, A.M.; Mancini, M.C.; Nie, S. Second Window for in Vivo Imaging. *Nat. Nanotechnol.* **2009**, *4*, 710–711. [CrossRef] [PubMed]
15. Wilhelm, S.; Tavares, A.J.; Dai, Q.; Ohta, S.; Audet, J.; Dvorak, H.F.; Chan, W.C.W. Analysis of Nanoparticle Delivery to Tumours. *Nat. Rev. Mater.* **2016**, *1*, 16014. [CrossRef]
16. Cheng, Y.-H.; He, C.; Riviere, J.E.; Monteiro-Riviere, N.A.; Lin, Z. Meta-Analysis of Nanoparticle Delivery to Tumors Using a Physiologically Based Pharmacokinetic Modeling and Simulation Approach. *ACS Nano* **2020**, *14*, 3075–3095. [CrossRef] [PubMed]
17. Sun, Q.; Zhou, Z.; Qiu, N.; Shen, Y. Rational Design of Cancer Nanomedicine: Nanoproperty Integration and Synchronization. *Adv. Mater.* **2017**, *29*, 1606628. [CrossRef] [PubMed]
18. Wayteck, L.; Dewitte, H.; De Backer, L.; Breckpot, K.; Demeester, J.; De Smedt, S.C.; Raemdonck, K. Hitchhiking Nanoparticles: Reversible Coupling of Lipid-Based Nanoparticles to Cytotoxic T Lymphocytes. *Biomaterials* **2016**, *77*, 243–254. [CrossRef] [PubMed]

19. Kydd, J.; Jadia, R.; Velpurisiva, P.; Gad, A.; Paliwal, S.; Rai, P. Targeting Strategies for the Combination Treatment of Cancer Using Drug Delivery Systems. *Pharmaceutics* **2017**, *9*, 46. [CrossRef]
20. Longmire, M.; Choyke, P.L.; Kobayashi, H. Clearance Properties of Nano-Sized Particles and Molecules as Imaging Agents: Considerations and Caveats. *Nanomedicine* **2008**, *3*, 703–717. [CrossRef]
21. Efremova, M.V.; Naumenko, V.A.; Spasova, M.; Garanina, A.S.; Abakumov, M.A.; Blokhina, A.D.; Melnikov, P.A.; Prelovskaya, A.O.; Heidelmann, M.; Li, Z.-A.; et al. Magnetite-Gold Nanohybrids as Ideal All-in-One Platforms for Theranostics. *Sci. Rep.* **2018**, *8*, 11295. [CrossRef] [PubMed]
22. Wei, W.; Zhang, X.; Chen, X.; Zhou, M.; Xu, R.; Zhang, X. Smart Surface Coating of Drug Nanoparticles with Cross-Linkable Polyethylene Glycol for Bio-Responsive and Highly Efficient Drug Delivery. *Nanoscale* **2016**, *8*, 8118–8125. [CrossRef] [PubMed]
23. Yetisgin, A.A.; Cetinel, S.; Zuvin, M.; Kosar, A.; Kutlu, O. Therapeutic Nanoparticles and Their Targeted Delivery Applications. *Molecules* **2020**, *25*, 2193. [CrossRef] [PubMed]
24. Junyaprasert, V.B.; Thummarati, P. Innovative Design of Targeted Nanoparticles: Polymer-Drug Conjugates for Enhanced Cancer Therapy. *Pharmaceutics* **2023**, *15*, 2216. [CrossRef] [PubMed]
25. Tawfik, S.M.; Azizov, S.; Elmasry, M.R.; Sharipov, M.; Lee, Y.-I. Recent Advances in Nanomicelles Delivery Systems. *Nanomaterials* **2020**, *11*, 70. [CrossRef] [PubMed]
26. Hu, H.; Masarapu, H.; Gu, Y.; Zhang, Y.; Yu, X.; Steinmetz, N.F. Physalis Mottle Virus-like Nanoparticles for Targeted Cancer Imaging. *ACS Appl. Mater. Interfaces* **2019**, *11*, 18213–18223. [CrossRef] [PubMed]
27. Shipunova, V.O.; Sogomonyan, A.S.; Zelepukin, I.V.; Nikitin, M.P.; Deyev, S.M. PLGA Nanoparticles Decorated with Anti-HER2 Affibody for Targeted Delivery and Photoinduced Cell Death. *Molecules* **2021**, *26*, 3955. [CrossRef] [PubMed]
28. Cohen, L.; Assaraf, Y.G.; Livney, Y.D. Novel Selectively Targeted Multifunctional Nanostructured Lipid Carriers for Prostate Cancer Treatment. *Pharmaceutics* **2021**, *14*, 88. [CrossRef]
29. Li, C.; Xiao, C.; Zhan, L.; Zhang, Z.; Xing, J.; Zhai, J.; Zhou, Z.; Tan, G.; Piao, J.; Zhou, Y.; et al. Wireless Electrical Stimulation at the Nanoscale Interface Induces Tumor Vascular Normalization. *Bioact. Mater.* **2022**, *18*, 399–408. [CrossRef]
30. Zhu, M.; Zhuang, J.; Li, Z.; Liu, Q.; Zhao, R.; Gao, Z.; Midgley, A.C.; Qi, T.; Tian, J.; Zhang, Z.; et al. Machine-Learning-Assisted Single-Vessel Analysis of Nanoparticle Permeability in Tumour Vasculatures. *Nat. Nanotechnol.* **2023**, *18*, 657–666. [CrossRef]
31. Wang, Q.; Liang, Q.; Dou, J.; Zhou, H.; Zeng, C.; Pan, H.; Shen, Y.; Li, Q.; Liu, Y.; Leong, D.T.; et al. Breaking through the Basement Membrane Barrier to Improve Nanotherapeutic Delivery to Tumours. *Nat. Nanotechnol.* **2023**, *19*, 95–105. [CrossRef] [PubMed]
32. Choi, Y.S.; Jang, H.; Gupta, B.; Jeong, J.-H.; Ge, Y.; Yong, C.S.; Kim, J.O.; Bae, J.-S.; Song, I.-S.; Kim, I.-S.; et al. Tie2-Mediated Vascular Remodeling by Ferritin-Based Protein C Nanoparticles Confers Antitumor and Anti-Metastatic Activities. *J. Hematol. Oncol.* **2020**, *13*, 123. [CrossRef] [PubMed]
33. Li, Y.; Miao, Y.; Chen, M.; Chen, X.; Li, F.; Zhang, X.; Gan, Y. Stepwise Targeting and Responsive Lipid-Coated Nanoparticles for Enhanced Tumor Cell Sensitivity and Hepatocellular Carcinoma Therapy. *Theranostics* **2020**, *10*, 3722–3736. [CrossRef] [PubMed]
34. Bugno, J.; Poellmann, M.J.; Sokolowski, K.; Hsu, H.; Kim, D.-H.; Hong, S. Tumor Penetration of Sub-10 Nm Nanoparticles: Effect of Dendrimer Properties on Their Penetration in Multicellular Tumor Spheroids. *Nanomed. Nanotechnol. Biol. Med.* **2019**, *21*, 102059. [CrossRef] [PubMed]
35. Li, M.; Zhang, Y.; Zhang, Q.; Li, J. Tumor Extracellular Matrix Modulating Strategies for Enhanced Antitumor Therapy of Nanomedicines. *Mater. Today Bio* **2022**, *16*, 100364. [CrossRef] [PubMed]
36. Durymanov, M.O.; Rosenkranz, A.A.; Sobolev, A.S. Current Approaches for Improving Intratumoral Accumulation and Distribution of Nanomedicines. *Theranostics* **2015**, *5*, 1007–1020. [CrossRef] [PubMed]
37. Yu, Z.; Gao, L.; Chen, K.; Zhang, W.; Zhang, Q.; Li, Q.; Hu, K. Nanoparticles: A New Approach to Upgrade Cancer Diagnosis and Treatment. *Nanoscale Res. Lett.* **2021**, *16*, 88. [CrossRef] [PubMed]
38. Bourquin, J.; Milosevic, A.; Hauser, D.; Lehner, R.; Blank, F.; Petri-Fink, A.; Rothen-Rutishauser, B. Biodistribution, Clearance, and Long-Term Fate of Clinically Relevant Nanomaterials. *Adv. Mater.* **2018**, *30*, 1704307. [CrossRef] [PubMed]
39. Wang, J.; Ni, Q.; Wang, Y.; Zhang, Y.; He, H.; Gao, D.; Ma, X.; Liang, X.-J. Nanoscale Drug Delivery Systems for Controllable Drug Behaviors by Multi-Stage Barrier Penetration. *J. Control. Release* **2021**, *331*, 282–295. [CrossRef]
40. Cheng, Q.; Shi, X.-L.; Li, Q.-L.; Wang, L.; Wang, Z. Current Advances on Nanomaterials Interfering with Lactate Metabolism for Tumor Therapy. *Adv. Sci.* **2024**, *11*, e2305662. [CrossRef]
41. Wu, W.; Pu, Y.; Shi, J. Nanomedicine-Enabled Chemotherapy-Based Synergetic Cancer Treatments. *J. Nanobiotechnol.* **2022**, *20*, 4. [CrossRef]
42. Ng, T.S.C.; Garlin, M.A.; Weissleder, R.; Miller, M.A. Improving Nanotherapy Delivery and Action through Image-Guided Systems Pharmacology. *Theranostics* **2020**, *10*, 968–997. [CrossRef] [PubMed]
43. Wang, Z.; Xue, X.; He, Y.; Lu, Z.; Jia, B.; Wu, H.; Yuan, Y.; Huang, Y.; Wang, H.; Lu, H.; et al. Novel Redox-Responsive Polymeric Magnetosomes with Tunable Magnetic Resonance Property for in Vivo Drug Release Visualization and Dual-Modal Cancer Therapy. *Adv. Funct. Mater.* **2018**, *28*, 1802159. [CrossRef]
44. Wu, L.; Wu, I.-C.; DuFort, C.C.; Carlson, M.A.; Wu, X.; Chen, L.; Kuo, C.-T.; Qin, Y.; Yu, J.; Hingorani, S.R.; et al. Photostable Ratiometric Pdot Probe for in Vitro and in Vivo Imaging of Hypochlorous Acid. *J. Am. Chem. Soc.* **2017**, *139*, 6911–6918. [CrossRef] [PubMed]
45. Tian, R.; Ma, H.; Zhu, S.; Lau, J.; Ma, R.; Liu, Y.; Lin, L.; Chandra, S.; Wang, S.; Zhu, X.; et al. Multiplexed NIR-II Probes for Lymph Node-Invaded Cancer Detection and Imaging-Guided Surgery. *Adv. Mater.* **2020**, *32*, 1907365. [CrossRef] [PubMed]

46. Hu, Z.; Feng, L.; Yang, P. 2, 1, 3-Benzothiadiazole Derivative Small Molecule Fluorophores for NIR-II Bioimaging. *Adv. Funct. Mater.* **2024**, *34*, 2310818. [CrossRef]
47. Liu, Y.; Li, Y.; Koo, S.; Sun, Y.; Liu, Y.; Liu, X.; Pan, Y.; Zhang, Z.; Du, M.; Lu, S.; et al. Versatile Types of Inorganic/Organic NIR-IIa/IIb Fluorophores: From Strategic Design toward Molecular Imaging and Theranostics. *Chem. Rev.* **2022**, *122*, 209–268. [CrossRef]
48. Li, C.; Chen, G.; Zhang, Y.; Wu, F.; Wang, Q. Advanced Fluorescence Imaging Technology in the Near-Infrared-II Window for Biomedical Applications. *J. Am. Chem. Soc.* **2020**, *142*, 14789–14804. [CrossRef]
49. Welsher, K.; Liu, Z.; Sherlock, S.P.; Robinson, J.T.; Chen, Z.; Daranciang, D.; Dai, H. A Route to Brightly Fluorescent Carbon Nanotubes for Near-Infrared Imaging in Mice. *Nat. Nanotechnol.* **2009**, *4*, 773–780. [CrossRef]
50. Welsher, K.; Sherlock, S.P.; Dai, H. Deep-Tissue Anatomical Imaging of Mice Using Carbon Nanotube Fluorophores in the Second Near-Infrared Window. *Proc. Natl. Acad. Sci. USA* **2011**, *108*, 8943–8948. [CrossRef]
51. Hong, G.; Lee, J.C.; Robinson, J.T.; Raaz, U.; Xie, L.; Huang, N.F.; Cooke, J.P.; Dai, H. Multifunctional in Vivo Vascular Imaging Using Near-Infrared II Fluorescence. *Nat. Med.* **2012**, *18*, 1841–1846. [CrossRef] [PubMed]
52. Majdinasab, M.; Mitsubayashi, K.; Marty, J.L. Optical and Electrochemical Sensors and Biosensors for the Detection of Quinolones. *Trends Biotechnol.* **2019**, *37*, 898–915. [CrossRef] [PubMed]
53. Xiao, M.; Lai, W.; Man, T.; Chang, B.; Li, L.; Chandrasekaran, A.R.; Pei, H. Rationally Engineered Nucleic Acid Architectures for Biosensing Applications. *Chem. Rev.* **2019**, *119*, 11631–11717. [CrossRef] [PubMed]
54. Chen, Z.; Wu, P.; Cong, R.; Xu, N.; Tan, Y.; Tan, C.; Jiang, Y. Sensitive Conjugated-Polymer-Based Fluorescent ATP Probes and Their Application in Cell Imaging. *ACS Appl. Mater. Interfaces* **2016**, *8*, 3567–3574. [CrossRef]
55. Du, Y.; Xu, B.; Fu, T.; Cai, M.; Li, F.; Zhang, Y.; Wang, Q. Near-Infrared Photoluminescent Ag_2S Quantum Dots from a Single Source Precursor. *J. Am. Chem. Soc.* **2010**, *132*, 1470–1471. [CrossRef]
56. Zhang, Y.; Hong, G.; Zhang, Y.; Chen, G.; Li, F.; Dai, H.; Wang, Q. Ag_2S Quantum Dot: A Bright and Biocompatible Fluorescent Nanoprobe in the Second Near-Infrared Window. *ACS Nano* **2012**, *6*, 3695–3702. [CrossRef] [PubMed]
57. Hong, G.; Robinson, J.T.; Zhang, Y.; Diao, S.; Antaris, A.L.; Wang, Q.; Dai, H. In Vivo Fluorescence Imaging with Ag_2S Quantum Dots in the Second Near-Infrared Region. *Angew. Chem. Int. Ed. Engl.* **2012**, *51*, 9818–9821. [CrossRef] [PubMed]
58. Yang, H.; Huang, H.; Ma, X.; Zhang, Y.; Yang, X.; Yu, M.; Sun, Z.; Li, C.; Wu, F.; Wang, Q. Au-Doped Ag_2Te Quantum Dots with Bright NIR-IIb Fluorescence for In Situ Monitoring of Angiogenesis and Arteriogenesis in a Hindlimb Ischemic Model. *Adv. Mater.* **2021**, *33*, 2103953. [CrossRef] [PubMed]
59. Dong, B.; Li, C.; Chen, G.; Zhang, Y.; Zhang, Y.; Deng, M.; Wang, Q. Facile Synthesis of Highly Photoluminescent Ag_2Se Quantum Dots as a New Fluorescent Probe in the Second Near-Infrared Window for in Vivo Imaging. *Chem. Mater.* **2013**, *25*, 2503–2509. [CrossRef]
60. Bruns, O.T.; Bischof, T.S.; Harris, D.K.; Franke, D.; Shi, Y.; Riedemann, L.; Bartelt, A.; Jaworski, F.B.; Carr, J.A.; Rowlands, C.J.; et al. Next-Generation in Vivo Optical Imaging with Short-Wave Infrared Quantum Dots. *Nat. Biomed. Eng.* **2017**, *1*, 0056. [CrossRef]
61. Yang, M.; Gui, R.; Jin, H.; Wang, Z.; Zhang, F.; Xia, J.; Bi, S.; Xia, Y. Ag_2Te Quantum Dots with Compact Surface Coatings of Multivalent Polymers: Ambient One-Pot Aqueous Synthesis and the Second Near-Infrared Bioimaging. *Colloids Surf. B Biointerfaces* **2015**, *126*, 115–120. [CrossRef] [PubMed]
62. Li, B.; Wang, G.; Tong, Y.; Zhang, Y.; Sun, S.-K.; Yu, C. Noninvasive Gastrointestinal Tract Imaging Using BSA-Ag_2Te Quantum Dots as a CT/NIR-II Fluorescence Dual-Modal Imaging Probe in Vivo. *ACS Biomater. Sci. Eng.* **2023**, *9*, 449–457. [CrossRef] [PubMed]
63. Li, Y.; Zeng, S.; Hao, J. Non-Invasive Optical Guided Tumor Metastasis/Vessel Imaging by Using Lanthanide Nanoprobe with Enhanced Down-Shifting Emission beyond 1500 Nm. *ACS Nano* **2019**, *13*, 248–259. [CrossRef] [PubMed]
64. Ren, F.; Li, T.; Yao, T.; Chen, G.; Li, C.; Wang, Q. Near-Infrared-II Fluorophores for In Vivo Multichannel Biosensing. *Chemosensors* **2023**, *11*, 433. [CrossRef]
65. Fan, Y.; Wang, P.; Lu, Y.; Wang, R.; Zhou, L.; Zheng, X.; Li, X.; Piper, J.A.; Zhang, F. Lifetime-Engineered NIR-II Nanoparticles Unlock Multiplexed In Vivo Imaging. *Nat. Nanotechnol.* **2018**, *13*, 941–946. [CrossRef] [PubMed]
66. Ren, F.; Huang, H.; Yang, H.; Xia, B.; Ma, Z.; Zhang, Y.; Wu, F.; Li, C.; He, T.; Wang, Q. Tailoring Near-Infrared-IIb Fluorescence of Thulium(III) by Nanocrystal Structure Engineering. *Nano Lett.* **2023**, *23*, 10058–10065. [CrossRef] [PubMed]
67. Zhu, X.; Wang, X.; Zhang, H.; Zhang, F. Luminescence Lifetime Imaging Based on Lanthanide Nanoparticles. *Angew. Chem. Int. Ed. Engl.* **2022**, *61*, e202209378. [CrossRef] [PubMed]
68. Dong, H.; Sun, L.-D.; Feng, W.; Gu, Y.; Li, F.; Yan, C.-H. Versatile Spectral and Lifetime Multiplexing Nanoplatform with Excitation Orthogonalized Upconversion Luminescence. *ACS Nano* **2017**, *11*, 3289–3297. [CrossRef]
69. Su, Y.; Yu, B.; Wang, S.; Cong, H.; Shen, Y. NIR-II Bioimaging of Small Organic Molecule. *Biomaterials* **2021**, *271*, 120717. [CrossRef]
70. Li, T.; Zhang, Y.; Wu, F.; Chen, G.; Li, C.; Wang, Q. Rational Design of NIR-II Ratiometric Fluorescence Probes for Accurate Bioimaging and Biosensing In Vivo. *Small Methods* **2024**, 2400132. [CrossRef]
71. Jiang, Z.; Ding, Y.; Lovell, J.F.; Zhang, Y. Design and Application of Organic Contrast Agents for Molecular Imaging in the Second Near Infrared (NIR-II) Window. *Photoacoustics* **2022**, *28*, 100426. [CrossRef] [PubMed]
72. Liu, X.; Yu, B.; Shen, Y.; Cong, H. Design of NIR-II High Performance Organic Small Molecule Fluorescent Probes and Summary of Their Biomedical Applications. *Coordin. Chem. Rev.* **2022**, *468*, 214609. [CrossRef]

73. Zhang, N.; Lu, C.; Chen, M.; Xu, X.; Shu, G.; Du, Y.; Ji, J. Recent Advances in Near-Infrared II Imaging Technology for Biological Detection. *J. Nanobiotechnol.* **2021**, *19*, 132. [CrossRef] [PubMed]
74. Zhou, J.; Ma, H. Design Principles of Spectroscopic Probes for Biological Applications. *Chem. Sci.* **2016**, *7*, 6309–6315. [CrossRef] [PubMed]
75. Huang, D.; Lin, S.; Wang, Q.; Zhang, Y.; Li, C.; Ji, R.; Wang, M.; Chen, G.; Wang, Q. An NIR-II Fluorescence/Dual Bioluminescence Multiplexed Imaging for In Vivo Visualizing the Location, Survival, and Differentiation of Transplanted Stem Cells. *Adv. Funct. Mater.* **2019**, *29*, 1806546. [CrossRef]
76. Hu, Z.; Fang, C.; Li, B.; Zhang, Z.; Cao, C.; Cai, M.; Su, S.; Sun, X.; Shi, X.; Li, C.; et al. First-in-Human Liver-Tumour Surgery Guided by Multispectral Fluorescence Imaging in the Visible and Near-Infrared-I/II Windows. *Nat. Biomed. Eng.* **2020**, *4*, 259–271. [CrossRef] [PubMed]
77. Hong, G.; Diao, S.; Chang, J.; Antaris, A.L.; Chen, C.; Zhang, B.; Zhao, S.; Atochin, D.N.; Huang, P.L.; Andreasson, K.I.; et al. Through-Skull Fluorescence Imaging of the Brain in a New Near-Infrared Window. *Nat. Photonics* **2014**, *8*, 723–730. [CrossRef] [PubMed]
78. Qi, J.; Sun, C.; Zebibula, A.; Zhang, H.; Kwok, R.T.K.; Zhao, X.; Xi, W.; Lam, J.W.Y.; Qian, J.; Tang, B.Z. Real-Time and High-Resolution Bioimaging with Bright Aggregation-Induced Emission Dots in Short-Wave Infrared Region. *Adv. Mater.* **2018**, *30*, e1706856. [CrossRef]
79. Chen, G.; Lin, S.; Huang, D.; Zhang, Y.; Li, C.; Wang, M.; Wang, Q. Revealing the Fate of Transplanted Stem Cells In Vivo with a Novel Optical Imaging Strategy. *Small* **2018**, *14*, 1702679. [CrossRef]
80. Wang, F.; Wan, H.; Ma, Z.; Zhong, Y.; Sun, Q.; Tian, Y.; Qu, L.; Du, H.; Zhang, M.; Li, L.; et al. Light-Sheet Microscopy in the Near-Infrared II Window. *Nat. Methods* **2019**, *16*, 545–552. [CrossRef]
81. Zhu, S.; Herraiz, S.; Yue, J.; Zhang, M.; Wan, H.; Yang, Q.; Ma, Z.; Wang, Y.; He, J.; Antaris, A.L.; et al. 3D NIR-II Molecular Imaging Distinguishes Targeted Organs with High-Performance NIR-II Bioconjugates. *Adv. Mater.* **2018**, *30*, 1705799. [CrossRef] [PubMed]
82. Wang, F.; Ma, Z.; Zhong, Y.; Salazar, F.; Xu, C.; Ren, F.; Qu, L.; Wu, A.M.; Dai, H. In Vivo NIR-II Structured-Illumination Light-Sheet Microscopy. *Proc. Natl. Acad. Sci. USA* **2021**, *118*, e2023888118. [CrossRef] [PubMed]
83. Mi, C.; Guan, M.; Zhang, X.; Yang, L.; Wu, S.; Yang, Z.; Guo, Z.; Liao, J.; Zhou, J.; Lin, F.; et al. High Spatial and Temporal Resolution NIR-IIb Gastrointestinal Imaging in Mice. *Nano Lett.* **2022**, *22*, 2793–2800. [CrossRef] [PubMed]
84. Liu, P.; Mu, X.; Zhang, X.-D.; Ming, D. The Near-Infrared-II Fluorophores and Advanced Microscopy Technologies Development and Application in Bioimaging. *Bioconjug. Chem.* **2020**, *31*, 260–275. [CrossRef] [PubMed]
85. Yang, S.; Cai, C.; Wang, H.; Ma, X.; Shao, A.; Sheng, J.; Yu, C. Drug Delivery Strategy in Hepatocellular Carcinoma Therapy. *Cell. Commun. Signal.* **2022**, *20*, 26. [CrossRef] [PubMed]
86. Le, Q.-V.; Lee, J.; Lee, H.; Shim, G.; Oh, Y.-K. Cell Membrane-Derived Vesicles for Delivery of Therapeutic Agents. *Acta Pharm. Sin. B* **2021**, *11*, 2096–2113. [CrossRef] [PubMed]
87. Li, C.; Li, F.; Zhang, Y.; Zhang, W.; Zhang, X.-E.; Wang, Q. Real-Time Monitoring Surface Chemistry-Dependent In Vivo Behaviors of Protein Nanocages via Encapsulating an NIR-II Ag_2S Quantum Dot. *ACS Nano* **2015**, *9*, 12255–12263. [CrossRef]
88. Li, Y.; Gao, J.; Wang, S.; Du, M.; Hou, X.; Tian, T.; Qiao, X.; Tian, Z.; Stang, P.J.; Li, S.; et al. Self-Assembled NIR-II Fluorophores with Ultralong Blood Circulation for Cancer Imaging and Image-Guided Surgery. *J. Med. Chem.* **2022**, *65*, 2078–2090. [CrossRef]
89. Li, S.; Chen, H.; Liu, H.; Liu, L.; Yuan, Y.; Mao, C.; Zhang, W.; Zhang, X.; Guo, W.; Lee, C.-S.; et al. In Vivo Real-Time Pharmaceutical Evaluations of Near-Infrared II Fluorescent Nanomedicine Bound Polyethylene Glycol Ligands for Tumor Photothermal Ablation. *ACS Nano* **2020**, *14*, 13681–13690. [CrossRef]
90. Ding, L.; Wu, Y.; Wu, M.; Zhao, Q.; Li, H.; Liu, J.; Liu, X.; Zhang, X.; Zeng, Y. Engineered Red Blood Cell Biomimetic Nanovesicle with Oxygen Self-Supply for Near-Infrared-II Fluorescence-Guided Synergetic Chemo-Photodynamic Therapy against Hypoxic Tumors. *ACS Appl. Mater. Interfaces* **2021**, *13*, 52435–52449. [CrossRef]
91. Yang, C.; Merlin, D. Nanoparticle-Mediated Drug Delivery Systems for The Treatment Of IBD: Current Perspectives. *Int. J. Nanomed.* **2019**, *14*, 8875–8889. [CrossRef] [PubMed]
92. Anwar, F.; Naqvi, S.; Shams, S.; Sheikh, R.A.; Al-Abbasi, F.A.; Asseri, A.H.; Baig, M.R.; Kumar, V. Nanomedicines: Intervention in Inflammatory Pathways of Cancer. *Inflammopharmacology* **2023**, *31*, 1199–1221. [CrossRef] [PubMed]
93. Golombek, S.K.; May, J.-N.; Theek, B.; Appold, L.; Drude, N.; Kiessling, F.; Lammers, T. Tumor Targeting via EPR: Strategies to Enhance Patient Responses. *Adv. Drug Deliv. Rev.* **2018**, *130*, 17–38. [CrossRef] [PubMed]
94. Luan, X.; Yuan, H.; Song, Y.; Hu, H.; Wen, B.; He, M.; Zhang, H.; Li, Y.; Li, F.; Shu, P.; et al. Reappraisal of Anticancer Nanomedicine Design Criteria in Three Types of Preclinical Cancer Models for Better Clinical Translation. *Biomaterials* **2021**, *275*, 120910. [CrossRef] [PubMed]
95. Song, C.; Zhang, Y.; Li, C.; Chen, G.; Kang, X.; Wang, Q. Enhanced Nanodrug Delivery to Solid Tumors Based on a Tumor Vasculature-Targeted Strategy. *Adv. Funct. Mater.* **2016**, *26*, 4192–4200. [CrossRef]
96. Wang, M.; Yan, D.; Wang, M.; Wu, Q.; Song, R.; Huang, Y.; Rao, J.; Wang, D.; Zhou, F.; Tang, B.Z. A Versatile 980 Nm Absorbing Aggregation-Induced Emission Luminogen for NIR-II Imaging-Guided Synergistic Photo-Immunotherapy Against Advanced Pancreatic Cancer. *Adv. Funct. Mater.* **2022**, *32*, 2205371. [CrossRef]
97. Liu, Q.; Tian, J.; Tian, Y.; Sun, Q.; Sun, D.; Liu, D.; Wang, F.; Xu, H.; Ying, G.; Wang, J.; et al. Thiophene Donor for NIR-II Fluorescence Imaging-Guided Photothermal/Photodynamic/Chemo Combination Therapy. *Acta Biomater.* **2021**, *127*, 287–297. [CrossRef]

98. Li, Y.; Fan, X.; Li, Y.; Zhu, L.; Chen, R.; Zhang, Y.; Ni, H.; Xia, Q.; Feng, Z.; Tang, B.Z.; et al. Biologically Excretable AIE Nanoparticles Wear Tumor Cell-Derived "Exosome Caps" for Efficient NIR-II Fluorescence Imaging-Guided Photothermal Therapy. *Nano Today* **2021**, *41*, 101333. [CrossRef]
99. Betancur, P.A.; Abraham, B.J.; Yiu, Y.Y.; Willingham, S.B.; Khameneh, F.; Zarnegar, M.; Kuo, A.H.; McKenna, K.; Kojima, Y.; Leeper, N.J.; et al. A CD47-Associated Super-Enhancer Links pro-Inflammatory Signalling to CD47 Upregulation in Breast Cancer. *Nat. Commun.* **2017**, *8*, 14802. [CrossRef]
100. Corma, A.; Botella, P.; Rivero-Buceta, E. Silica-Based Stimuli-Responsive Systems for Antitumor Drug Delivery and Controlled Release. *Pharmaceutics* **2022**, *14*, 110. [CrossRef]
101. Chen, M.; Cui, Y.; Hao, W.; Fan, Y.; Zhang, J.; Liu, Q.; Jiang, M.; Yang, Y.; Wang, Y.; Gao, C. Ligand-Modified Homologous Targeted Cancer Cell Membrane Biomimetic Nanostructured Lipid Carriers for Glioma Therapy. *Drug Deliv.* **2021**, *28*, 2241–2255. [CrossRef]
102. Zhang, X.; He, S.; Ding, B.; Qu, C.; Zhang, Q.; Chen, H.; Sun, Y.; Fang, H.; Long, Y.; Zhang, R.; et al. Cancer Cell Membrane-Coated Rare Earth Doped Nanoparticles for Tumor Surgery Navigation in NIR-II Imaging Window. *Chem. Eng. J.* **2020**, *385*, 123959. [CrossRef]
103. Zhang, J.-J.; Lin, Y.; Zhou, H.; He, H.; Ma, J.-J.; Luo, M.-Y.; Zhang, Z.-L.; Pang, D.-W. Cell Membrane-Camouflaged NIR II Fluorescent Ag_2Te Quantum Dots-Based Nanobioprobes for Enhanced In Vivo Homotypic Tumor Imaging. *Adv. Healthc. Mater.* **2019**, *8*, e1900341. [CrossRef] [PubMed]
104. Pegtel, D.M.; Gould, S.J. Exosomes. *Annu. Rev. Biochem.* **2019**, *88*, 487–514. [CrossRef] [PubMed]
105. Chen, H.; Shou, K.; Chen, S.; Qu, C.; Wang, Z.; Jiang, L.; Zhu, M.; Ding, B.; Qian, K.; Ji, A.; et al. Smart Self-Assembly Amphiphilic Cyclopeptide-Dye for Near-Infrared Window-II Imaging. *Adv. Mater.* **2021**, *33*, 2006902. [CrossRef]
106. Li, S.; Zhang, Y.; Liu, X.; Tian, Y.; Cheng, Y.; Tang, L.; Lin, H. Smart NIR-II Croconaine Dye-Peptide for Enhanced Photo-Sonotheranostics of Hepatocellular Carcinoma. *Theranostics* **2022**, *12*, 76–86. [CrossRef] [PubMed]
107. Munir, M.U. Nanomedicine Penetration to Tumor: Challenges, and Advanced Strategies to Tackle This Issue. *Cancers* **2022**, *14*, 2904. [CrossRef] [PubMed]
108. Yan, M.; Chen, Q.; Liu, T.; Li, X.; Pei, P.; Zhou, L.; Zhou, S.; Zhang, R.; Liang, K.; Dong, J.; et al. Site-Selective Superassembly of Biomimetic Nanorobots Enabling Deep Penetration into Tumor with Stiff Stroma. *Nat. Commun.* **2023**, *14*, 4628. [CrossRef]
109. Bugno, J.; Hsu, H.-J.; Pearson, R.M.; Noh, H.; Hong, S. Size and Surface Charge of Engineered Poly(Amidoamine) Dendrimers Modulate Tumor Accumulation and Penetration: A Model Study Using Multicellular Tumor Spheroids. *Mol. Pharm.* **2016**, *13*, 2155–2163. [CrossRef]
110. Han, Y.; Liu, H.; Fan, M.; Gao, S.; Fan, D.; Wang, Z.; Chang, J.; Zhang, J.; Ge, K. Near-Infrared-II Photothermal Ultra-Small Carbon Dots Promoting Anticancer Efficiency by Enhancing Tumor Penetration. *J. Colloid. Interf. Sci.* **2022**, *616*, 595–604. [CrossRef]
111. Wei, D.; Yu, Y.; Huang, Y.; Jiang, Y.; Zhao, Y.; Nie, Z.; Wang, F.; Ma, W.; Yu, Z.; Huang, Y.; et al. A Near-Infrared-II Polymer with Tandem Fluorophores Demonstrates Superior Biodegradability for Simultaneous Drug Tracking and Treatment Efficacy Feedback. *ACS Nano* **2021**, *15*, 5428–5438. [CrossRef] [PubMed]
112. Yang, X.; Li, C.; Yang, H.; Li, T.; Ling, S.; Zhang, Y.; Wu, F.; Liu, X.; Liu, S.; Fan, C.; et al. Programmed Remodeling of the Tumor Milieu to Enhance NK Cell Immunotherapy Combined with Chemotherapy for Pancreatic Cancer. *Nano Lett.* **2024**, *24*, 3421–3431. [CrossRef]
113. Jia, R.; Teng, L.; Gao, L.; Su, T.; Fu, L.; Qiu, Z.; Bi, Y. Advances in Multiple Stimuli-Responsive Drug-Delivery Systems for Cancer Therapy. *Int. J. Nanomed.* **2021**, *16*, 1525–1551. [CrossRef] [PubMed]
114. Chen, B.; Dai, W.; He, B.; Zhang, H.; Wang, X.; Wang, Y.; Zhang, Q. Current Multistage Drug Delivery Systems Based on the Tumor Microenvironment. *Theranostics* **2017**, *7*, 538–558. [CrossRef]
115. Khawar, I.A.; Kim, J.H.; Kuh, H.-J. Improving Drug Delivery to Solid Tumors: Priming the Tumor Microenvironment. *J. Control. Release* **2015**, *201*, 78–89. [CrossRef]
116. Haider, T.; Sandha, K.K.; Soni, V.; Gupta, P.N. Recent Advances in Tumor Microenvironment Associated Therapeutic Strategies and Evaluation Models. *Mater. Sci. Eng. C* **2020**, *116*, 111229. [CrossRef]
117. Loria, R.; Giliberti, C.; Bedini, A.; Palomba, R.; Caracciolo, G.; Ceci, P.; Falvo, E.; Marconi, R.; Falcioni, R.; Bossi, G.; et al. Very Low Intensity Ultrasounds as a New Strategy to Improve Selective Delivery of Nanoparticles-Complexes in Cancer Cells. *J. Exp. Clin. Cancer Res.* **2019**, *38*, 1. [CrossRef] [PubMed]
118. Ha, M.K.; Chung, K.H.; Yoon, T.H. Heterogeneity in Biodistribution and Cytotoxicity of Silver Nanoparticles in Pulmonary Adenocarcinoma Human Cells. *Nanomaterials* **2019**, *10*, 36. [CrossRef]
119. Choi, G.; Rejinold, N.S.; Piao, H.; Choy, J.-H. Inorganic-Inorganic Nanohybrids for Drug Delivery, Imaging and Photo-Therapy: Recent Developments and Future Scope. *Chem. Sci.* **2021**, *12*, 5044–5063. [CrossRef]
120. Azizi, M.; Jahanban-Esfahlan, R.; Samadian, H.; Hamidi, M.; Seidi, K.; Dolatshahi-Pirouz, A.; Yazdi, A.A.; Shavandi, A.; Laurent, S.; Be Omide Hagh, M.; et al. Multifunctional Nanostructures: Intelligent Design to Overcome Biological Barriers. *Mater. Today Bio.* **2023**, *20*, 100672. [CrossRef]
121. Sohrabi Kashani, A.; Packirisamy, M. Cancer-Nano-Interaction: From Cellular Uptake to Mechanobiological Responses. *Int. J. Mol. Sci.* **2021**, *22*, 9587. [CrossRef]
122. Antaris, A.L.; Chen, H.; Cheng, K.; Sun, Y.; Hong, G.; Qu, C.; Diao, S.; Deng, Z.; Hu, X.; Zhang, B.; et al. A Small-Molecule Dye for NIR-II Imaging. *Nat. Mater.* **2016**, *15*, 235–242. [CrossRef] [PubMed]

123. Wang, W.; Ma, Z.; Zhu, S.; Wan, H.; Yue, J.; Ma, H.; Ma, R.; Yang, Q.; Wang, Z.; Li, Q.; et al. Molecular Cancer Imaging in the Second Near-Infrared Window Using a Renal-Excreted NIR-II Fluorophore-Peptide Probe. *Adv. Mater.* **2018**, *30*, 1800106. [CrossRef]
124. Wen, Q.; Zhang, Y.; Li, C.; Ling, S.; Yang, X.; Chen, G.; Yang, Y.; Wang, Q. NIR-II Fluorescent Self-Assembled Peptide Nanochain for Ultrasensitive Detection of Peritoneal Metastasis. *Angew. Chem. Int. Ed. Engl.* **2019**, *58*, 11001–11006. [CrossRef] [PubMed]
125. Yuan, Y.; Diao, S.; Ni, X.; Zhang, D.; Yi, W.; Jian, C.; Hu, X.; Li, D.; Yu, A.; Zhou, W.; et al. Peptide-Based Semiconducting Polymer Nanoparticles for Osteosarcoma-Targeted NIR-II Fluorescence/NIR-I Photoacoustic Dual-Model Imaging and Photothermal/Photodynamic Therapies. *J. Nanobiotechnol.* **2022**, *20*, 44. [CrossRef] [PubMed]
126. Zhang, X.; Wan, J.; Mo, F.; Tang, D.; Xiao, H.; Li, Z.; Jia, J.; Liu, T. Targeting Bone Tumor and Subcellular Endoplasmic Reticulum via Near Infrared II Fluorescent Polymer for Photodynamic-Immunotherapy to Break the Step-Reduction Delivery Dilemma. *Adv. Sci.* **2022**, *9*, 2201819. [CrossRef] [PubMed]
127. He, Y.; Wang, S.; Yu, P.; Yan, K.; Ming, J.; Yao, C.; He, Z.; El-Toni, A.M.; Khan, A.; Zhu, X.; et al. NIR-II Cell Endocytosis-Activated Fluorescent Probes for in Vivo High-Contrast Bioimaging Diagnostics. *Chem. Sci.* **2021**, *12*, 10474–10482. [CrossRef]
128. Wei, X.; Song, M.; Jiang, G.; Liang, M.; Chen, C.; Yang, Z.; Zou, L. Progress in Advanced Nanotherapeutics for Enhanced Photodynamic Immunotherapy of Tumor. *Theranostics* **2022**, *12*, 5272–5298. [CrossRef]
129. Dasgupta, A.; Biancacci, I.; Kiessling, F.; Lammers, T. Imaging-Assisted Anticancer Nanotherapy. *Theranostics* **2020**, *10*, 956–967. [CrossRef]
130. Mishra, S.; Bhatt, T.; Kumar, H.; Jain, R.; Shilpi, S.; Jain, V. Nanoconstructs for Theranostic Application in Cancer: Challenges and Strategies to Enhance the Delivery. *Front. Pharmacol.* **2023**, *14*, 1101320. [CrossRef]
131. Liu, K.; Yao, Y.; Xue, S.; Zhang, M.; Li, D.; Xu, T.; Zhi, F.; Liu, Y.; Ding, D. Recent Advances of Tumor Microenvironment-Responsive Nanomedicines-Energized Combined Phototherapy of Cancers. *Pharmaceutics* **2023**, *15*, 2480. [CrossRef] [PubMed]
132. Wang, R.; Zhou, L.; Wang, W.; Li, X.; Zhang, F. In Vivo Gastrointestinal Drug-Release Monitoring through Second Near-Infrared Window Fluorescent Bioimaging with Orally Delivered Microcarriers. *Nat. Commun.* **2017**, *8*, 14702. [CrossRef] [PubMed]
133. Ling, S.; Yang, X.; Li, C.; Zhang, Y.; Yang, H.; Chen, G.; Wang, Q. Tumor Microenvironment-Activated NIR-II Nanotheranostic System for Precise Diagnosis and Treatment of Peritoneal Metastasis. *Angew. Chem. Int. Edit.* **2020**, *59*, 7219–7223. [CrossRef] [PubMed]
134. Tang, D.; Yu, Y.; Zhang, J.; Dong, X.; Liu, C.; Xiao, H. Self-Sacrificially Degradable Pseudo-Semiconducting Polymer Nanoparticles That Integrate NIR-II Fluorescence Bioimaging, Photodynamic Immunotherapy, and Photo-Activated Chemotherapy. *Adv. Mater.* **2022**, *34*, 2203820. [CrossRef]
135. Xie, Q.; Liu, J.; Chen, B.; Ge, X.; Zhang, X.; Gao, S.; Ma, Q.; Song, J. NIR-II Fluorescent Activatable Drug Delivery Nanoplatform for Cancer-Targeted Combined Photodynamic and Chemotherapy. *ACS Appl. Bio Mater.* **2022**, *5*, 711–722. [CrossRef] [PubMed]
136. Dai, Y.; Zhang, F.; Chen, K.; Sun, Z.; Wang, Z.; Xue, Y.; Li, M.; Fan, Q.; Shen, Q.; Zhao, Q. An Activatable Phototheranostic Nanoplatform for Tumor Specific NIR-II Fluorescence Imaging and Synergistic NIR-II Photothermal-Chemodynamic Therapy. *Small* **2023**, *19*, 2206053. [CrossRef] [PubMed]
137. Chen, T.; Hou, P.; Zhang, Y.; Ao, R.; Su, L.; Jiang, Y.; Zhang, Y.; Cai, H.; Wang, J.; Chen, Q.; et al. Singlet Oxygen Generation in Dark-Hypoxia by Catalytic Microenvironment-Tailored Nanoreactors for NIR-II Fluorescence-Monitored Chemodynamic Therapy. *Angew. Chem. Int. Ed. Engl.* **2021**, *60*, 15006–15012. [CrossRef] [PubMed]
138. Fu, Q.; Feng, H.; Su, L.; Zhang, X.; Liu, L.; Fu, F.; Yang, H.; Song, J. An Activatable Hybrid Organic–Inorganic Nanocomposite as Early Evaluation System of Therapy Effect. *Angew. Chem. Int. Ed. Engl.* **2022**, *61*, e202112237. [CrossRef]
139. Su, L.; Chen, Y.; Huo, H.; Liao, N.; Wu, Y.; Ge, X.; Guo, Z.; Chen, Z.; Zhang, X.; Song, J. NIR-II Ratiometric Chemiluminescent/Fluorescent Reporters for Real-Time Monitoring and Evaluating Cancer Photodynamic Therapy Efficacy. *Small* **2022**, *18*, 2202551. [CrossRef]
140. Yuan, M.; Fang, X.; Liu, J.; Yang, K.; Xiao, S.; Yang, S.; Du, W.; Song, J. NIR-II Self-Luminous Molecular Probe for In Vivo Inflammation Tracking and Cancer PDT Effect Self-Evaluating. *Small* **2023**, *19*, 2206666. [CrossRef]
141. Kim, H.S.; Lee, D.Y. Nanomedicine in Clinical Photodynamic Therapy for the Treatment of Brain Tumors. *Biomedicines* **2022**, *10*, 96. [CrossRef] [PubMed]
142. Xiao, F.; Lin, L.; Chao, Z.; Shao, C.; Chen, Z.; Wei, Z.; Lu, J.; Huang, Y.; Li, L.; Liu, Q.; et al. Organic Spherical Nucleic Acids for the Transport of a NIR-II-Emitting Dye Across the Blood-Brain Barrier. *Angew. Chem. Int. Ed. Engl.* **2020**, *59*, 9702–9710. [CrossRef] [PubMed]
143. Li, C.; Zhang, Y.; Chen, G.; Hu, F.; Zhao, K.; Wang, Q. Engineered Multifunctional Nanomedicine for Simultaneous Stereotactic Chemotherapy and Inhibited Osteolysis in an Orthotopic Model of Bone Metastasis. *Adv. Mater.* **2017**, *29*, 1605754. [CrossRef] [PubMed]